Journal of Integrative Neuroscience

J. Integr. Neurosci. **2026**; 25(11): 55213
https://doi.org/10.31083/JIN55213

Original Research

Rosmarinic Acid Targets Gamma-Radiation-Induced Cerebellar Oxidative Stress, Inflammation, and Apoptosis via Interplay Between Nrf2/HO-1 and NF-κB/NLRP3 Pathways: A Combined *in Vivo* and *in Silico* Study

Ahmed Alzahrani[1], Medhat Taha[2,3,*], Naeem F. Qusty[4], Bayan T. Bokhari[4], Tourki A.S. Baokbah[5], Omar Babateen[6], Alaa Jameel A. Albarakati[7], Turki M. Alharthi[4]

[1]Department of Biochemistry, Al-Qunfudah Medical College, Umm Al-Qura University, 21955 Makkah, Saudi Arabia
[2]Department of Anatomy and Embryology, Faculty of Medicine, Mansoura University, 35516 Mansoura, Egypt
[3]Department of Anatomy, Al-Qunfudah Medical College, Umm Al-Qura University, 28821 Al-Qunfudhah, Saudi Arabia
[4]Department of Clinical Laboratory Sciences, Faculty of Applied Medical Sciences, Umm Al-Qura University, 21955 Makkah, Saudi Arabia
[5]Department of Medical Emergency Services, College of Health Sciences-Al-Qunfudah, Umm Al-Qura University, 28821 Al-Qunfudah, Saudi Arabia
[6]Department of Physiology, Faculty of Medicine, Umm Al-Qura University, 21955 Makkah, Saudi Arabia
[7]Surgery Department, College of Medicine, Al-Qunfudah Branch, Umm Al-Qura University, 21955 Makkah, Saudi Arabia
*Correspondence: medhattaha53@yahoo.com (Medhat Taha)
Academic Editor: Mahmoud M. Iravani
Submitted: 24 June 2026 Revised: 8 September 2026 Accepted: 18 September 2026 Published: 17 November 2026

Abstract

Background: Radiotherapy (RT) is a crucial modality in the treatment of malignancies; however, its use may inadvertently cause cerebellar injury due to its neurotoxic effects. This study aimed to evaluate the radioprotective potential of rosmarinic acid (RA) against gamma radiation (GR)-induced cerebellar toxicity in experimental rats. **Methods:** Forty rats were randomly divided into four groups: the control group, which received saline for 14 days; the RA group, which received RA orally at a dose of 120 mg/kg/day; the GR group, which was exposed to a single whole-body dose of 6 Gy; and the GR+RA group, which received 6 Gy of whole-body GR followed by RA administration at the same dose for 14 days. Cerebellar tissues underwent histopathological evaluation. Oxidative stress markers, including malondialdehyde (MDA), superoxide dismutase (SOD), catalase (CAT), and glutathione (GSH), were determined using their respective colorimetric and spectrophotometric assays. Enzyme-linked immunosorbent assay (ELISA) was used to quantify NLRP3, IL-1β, IL-6, and IL-18. Immunohistochemistry (IHC) was performed to evaluate the expression of glial fibrillary acidic protein (GFAP), caspase-3, caspase-1, and tumor necrosis factor-alpha (TNF-α). Quantitative reverse transcription polymerase chain reaction (qRT-PCR) was performed to assess the gene expression of nuclear factor erythroid 2-related factor 2 (*Nrf2*), heme oxygenase-1 (*HO-1*), nuclear factor kappa-B (*NF-κB*), Bcl-2-associated X protein (*Bax*), and B-cell lymphoma 2 (*Bcl-2*). **Results:** The findings revealed that RA conferred protection against GR-induced cerebellar injury by mitigating oxidative stress through upregulation of the Nrf2 pathway, which enhanced antioxidant levels and reduced lipid peroxidation. This effect was mechanistically supported by molecular docking showing RA's strong binding to Keap1, suggesting disruption of the Keap1–Nrf2 complex and subsequent Nrf2 nuclear translocation. In addition, RA diminished radiation-induced inflammation by suppressing the NF-κB signaling pathway, thereby decreasing pro-inflammatory cytokines (TNF-α, IL-1β, and IL-6) and inhibiting the NLR family pyrin domain-containing 3 (NLRP3)/caspase-1 pyroptotic pathway (NLRP3, caspase-1, IL-1β, and IL-18). The anti-inflammatory effect was further corroborated by RA's favorable binding to inhibitor of nuclear factor kappa-B kinase subunit beta (IKKβ), indicating potential inhibition of NF-κB activation. Moreover, RA exhibited anti-apoptotic effects by downregulating caspase-3 and Bax while increasing Bcl-2 expression, resulting in substantial improvement in cerebellar histological architecture. The rotarod assessment confirmed that GR severely impaired motor equilibrium, whereas post-irradiation RA treatment markedly restored balance performance, indicating functional recovery that aligned with the observed histomorphological preservation. The anti-apoptotic activity was supported by molecular docking demonstrating robust binding of RA to caspase-3, suggesting a direct modulatory effect on the apoptotic cascade. **Conclusions:** These results underscore the therapeutic potential of RA in mitigating RT-induced cerebellar degeneration and emphasize the need for further research to translate these benefits into clinical oncology practice.

Keywords: rosmarinic acid; cerebellum; radiation; ionizing; oxidative stress; inflammation; pyroptosis; apoptosis

Copyright: © 2026 The Author(s). Published by IMR Press.
This is an open access article under the CC BY 4.0 license.

Publisher's Note: IMR Press stays neutral with regard to jurisdictional claims in published maps and institutional affiliations.

1. Introduction

The incidence and mortality of cancer have increased globally. According to Sung et al. [1] and Bray et al. [2], 19.3 million individuals were newly diagnosed with cancer, and approximately 10 million die annually from the disease. Radiotherapy (RT) is one of the established cancer treatments, frequently used in combination with chemotherapy and surgery [3,4,5]. RT is included in the treatment regimen for more than half of cancer patients [6,7]. Ionizing radiation primarily exerts its effects by damaging the DNA of cancer cells, causing single- or double-strand breaks and cross-link formation [8]. A significant challenge in RT is accurately targeting malignant tissues while minimizing harm to surrounding healthy tissues [9,10,11]. For example, irradiation of nasopharyngeal, hypopharyngeal, and cervical lymph node cancers can affect nearby nervous system structures, potentially causing severe neuronal damage that presents as cerebellar neuronal loss, radiation myelopathy, or encephalopathy [12,13,14].

Oxidative stress is a well-recognized mechanism in irradiation pathology [15]. Cell membranes in all aerobic organisms are highly vulnerable to damage caused by reactive oxygen species (ROS), including free radicals (FRs) such as hydroxyl, superoxide, and peroxyl radicals, as well as non-radicals like hydrogen peroxide, ozone, peroxynitrite, hypochlorous acid, and singlet oxygen [16]. Moreover, excess FRs react with polyunsaturated fatty acids (PUFAs) in cellular membranes, initiating oxidative degradation of lipids. Nervous tissue, being rich in PUFAs, is particularly susceptible to radiation-induced degeneration, which can manifest as arterial wall thickening, endothelial loss, demyelination, destructive glial reactions, telangiectasia, and thrombosis [17,18].

Gamma radiation (GR) activates the nuclear factor kappa-B (NF-κB) signaling pathway through multiple mechanisms [19,20,21,22], playing a critical role in regulating the survival and death of irradiated cells. Additionally, ionizing radiation (IR) stimulates several intracellular nucleotide-binding oligomerization domain (NOD)-like receptor proteins, leading to the formation of inflammasome complexes (NLRP1/NLR family pyrin domain-containing 3 (NLRP3)). This activation subsequently triggers caspase-1, a key protease that promotes the secretion of cytokines interleukin-1 beta (IL-1β) and interleukin-18 (IL-18) [23]. NF-κB further regulates the activation of NLRP3, IL-1β, and IL-18, thereby amplifying inflammatory responses [24]. Moreover, Nuclear factor erythroid 2-related factor 2 (Nrf2), a crucial transcription factor, mitigates oxidative stress by upregulating genes that encode components of the antioxidant defense system. In addition to its antioxidative role, Nrf2 protects cells against inflammatory injury, emphasizing its importance in cellular defense mechanisms [25]. The functional antagonism between Nrf2 and NF-κB establishes a regulatory rheostat wherein Nrf2-mediated antioxidant gene expression counterbalances NF-κB-driven inflammatory responses. Radiation disrupts this equilibrium by promoting NF-κB dominance through ROS-dependent IKK activation while simultaneously suppressing Nrf2 transcriptional activity [26,27]. Furthermore, recent evidence demonstrates that radiation-induced ROS and DNA damage activate the NLRP3 inflammasome through NF-κB-dependent priming, followed by mitochondrial damage releasing oxidized mtDNA as NLRP3 agonists, leading to caspase-1-mediated pyroptosis [26].

Rosmarinic acid (RA), an active constituent of *S. glabra*, is a water-soluble phenolic compound [28] known for its therapeutic properties, including anti-inflammatory, anti-angiogenic, and anticancer activities [29,30,31]. The antioxidant function of RA is critical in preventing FRs' interactions with membrane PUFAs, thereby inhibiting lipid peroxidation and halting chain reactions [32]. Research indicated that RA exhibits strong scavenging activity against radiation-induced ROS, effectively preventing FR-mediated cellular damage. It has demonstrated superior antioxidant efficacy compared with folic acid, caffeic acid, and chlorogenic acid [33,34]. Furthermore, previous studies have reported its radioprotective effects against IR-induced cellular injury [35].

This study aimed to investigate the neuroprotective effects of RA against GR-induced cerebellar injury and to elucidate the potential underlying mechanisms *in vivo*. The investigation included histological analysis, assessment of oxidative stress markers (malondialdehyde (MDA), superoxide dismutase (SOD), catalase (CAT), and glutathione (GSH)), evaluation of Nrf2/Heme oxygenase-1 (HO-1) pathway components, quantification of inflammatory markers (NF-κB, tumor necrosis factor-alpha (TNF-α), IL-6, and IL-1β), examination of the NLRP3/caspase-1/IL-1β pathway, and determination of neuronal survival indicators (caspase-3, Bcl-2-associated X protein (Bax), and B-cell lymphoma 2 (Bcl-2)) in cerebellar tissues following GR exposure. Additionally, molecular docking simulations were employed to predict the binding interactions of RA with key target proteins—Keap1, inhibitor of nuclear factor kappa-B kinase subunit beta (IKKβ), and caspase-3—to provide structural insights into its antioxidant, anti-inflammatory, and anti-apoptotic mechanisms. This study represents the inaugural investigation into RA-mediated neuroprotection of cerebellar tissue following GR. The multidisciplinary approach encompassing biochemical assays, histological examination, behavioral testing, and *in silico* docking revealed the intricate crosstalk between Nrf2-driven antioxidant defense and NF-κB/NLRP3-mediated inflammatory responses in radiation-induced cerebellar damage. These observations lay the groundwork for clinical translation of RA as a radioprotective adjuvant.

2. Materials and Methods

2.1 Experimental Animals

Forty male Wistar rats, aged 10 weeks and weighing 150–200 g, were used in this study. The animals were acclimated for 15 days before the experiment began to ensure proper adaptation. They were provided with unrestricted access to food and water daily. Housing conditions were maintained in polycarbonate cages at a temperature of 21–24 °C, with 50% relative humidity and a 12-hour light/-dark cycle. Approval was granted by the Ethics Committee of Umm Al-Qura University, Makka, Saudi Arabia (No HAPO-02-K-012-2025-06-2850).

2.2 Gamma Irradiation

Cerebellar injury was induced in rats using a single 6 Gy whole-body GR dose delivered at 0.48 Gy/min, using a Gamma Cell-40 biological irradiator containing a ^{137}Cs source. During treatment, rats were housed in plastic containers attached to the irradiator chamber. The 6 Gy dose was selected based on established protocols from previous research [36].

2.3 Experimental Design

The animals were randomly divided into four groups (n = 10 per group). The control group received normal saline via oral gavage daily for 14 days. In the RA group (Group II), rats were administered RA at a dose of 120 mg/kg/day (Catalog No. R4035; Sigma-Aldrich, St. Louis, MO, USA), dissolved in normal saline and given by oral gavage for 14 consecutive days. This neuroprotective dose was selected based on the study by Zhang et al. [37]. The GR group (Group III) received normal saline throughout the experimental period and was exposed to a single dose of GR (6 Gy) on day 1, as described in the protocol by Khateeb [36]. The GR+RA group (Group IV) was exposed to 6 Gy of GR on day 1, followed by oral administration of RA at the same dose and route for 14 days.

2.4 Behavioral Test

Motor function in laboratory rodents was evaluated using the rotarod apparatus, which consists of a rotating cylinder. The test quantifies the duration that an animal remains atop the revolving rod as a function of rotational velocity. Prior to data collection, rats underwent a training regimen to achieve stable performance, defined as maintaining balance on the rod for a minimum of 60 seconds at a fixed speed of 12 rpm. This criterion had to be met across three consecutive trials, with a 5-minute rest period allotted between each attempt. To prevent olfactory cues from influencing subsequent subjects, the equipment was thoroughly cleansed after every animal was tested. The final outcome measure for each rat was the mean latency to fall, calculated from the three successful trials [38].

2.5 Tissue Collection

After performing the behavioral examination, the animals were anesthetized via intraperitoneal injection of ketamine (50 mg/kg)/xylazine (5 mg/kg). Adequate anesthetic depth was confirmed before euthanasia by the absence of the pedal withdrawal reflex [39]. The animals were then euthanized by cervical dislocation. A midline incision was made to excise the cerebellum, which was subsequently divided into two parts. One portion was homogenized (1:10 w/v) in ice-cold 1.15% KCl buffer (pH = 7.2), centrifuged at 5000 rpm for 15 minutes at 4 °C, and the resulting supernatant was stored at –80 °C for biochemical and molecular analyses. Cerebellar tissue homogenates were prepared at a standardized ratio of 1:10 (w/v) in ice-cold 1.15% KCl buffer. To ensure consistency across samples, all tissue specimens were weighed prior to homogenization, and the homogenization volume was adjusted accordingly based on tissue weight. This standardized protocol minimizes variability arising from differences in tissue sampling weight. The second portion was fixed in 10% neutral buffered formalin for histological and immunohistochemical assessment.

2.6 Biochemical Analysis

Cerebellar supernatant was utilized to determine the concentration of the lipid peroxidation marker MDA following the method of Mihara and Uchiyama [40], using an Enzyme-linked immunosorbent assay (ELISA) reader at 540 nm. The activity of SOD was measured according to the procedure described by Marklund and Marklund [41]. Catalase (CAT) activity was determined spectrophotometrically at 240 nm by measuring the rate of H_2O_2 degradation, as outlined by Oberley and Spitz [42]. Additionally, GSH content was quantified following the method reported by Ellman [43]. MDA and GSH contents were expressed as nmol/g wet tissue, whereas SOD and CAT activities were expressed as U/mg protein. Tissue homogenates were prepared at a standardized 1:10 (w/v) ratio, ensuring consistent dilution across all samples.

2.7 ELISA Assay

In this study, commercially available ELISA kits were employed to quantify the pyroptosis markers IL-18, and NLRP3 (Cat. # EK720281 and EK247060; AFG Bioscience, Northbrook, IL, USA), as well as the pro-inflammatory cytokines IL-1β and IL-6 (Cat. # ELK1272 and ELK1158; ELK Biotechnology Co., Denver, CO, USA). All assays were conducted in accordance with the manufacturers' instructions to ensure accuracy and reproducibility.

2.8 Histopathological Examination

Following euthanasia by cervical dislocation under the anesthesia protocol described in Section 2.5, the skull was opened and the cerebellum was carefully excised from each

animal (n = 10 per group). The portion designated for histological and immunohistochemical assessment was immersed in 10% neutral buffered formalin (pH = 7.4) for 24 hours to ensure proper fixation. The fixed tissues were subsequently embedded in paraffin blocks. Sections (4.5-µm thick) were prepared and stained with hematoxylin and eosin (H&E) for histological evaluation under a light microscope.

2.9 Immunohistochemical Evaluation

Immunohistochemical analysis was conducted to assess the expression of cerebellar proteins TNF-α, glial fibrillary acidic protein (GFAP), caspase-3, and caspase-1, following previously established procedures [44]. Five-micrometer sections were deparaffinized and subjected to antigen retrieval. Endogenous peroxidase activity was blocked using hydrogen peroxide solution, after which non-specific binding was minimized with 5% bovine serum albumin in a humidified chamber. The sections were incubated overnight at 4 °C with primary antibodies: anti-caspase-3 (1:500 dilution; Cat. # CPP32 4-1-18; Thermo Fisher Scientific, Fremont, CA, USA), anti-caspase-1 (1:500 dilution; Cat. # MA5-16215; Thermo Fisher Scientific, Fremont, CA, USA), anti-TNF-α (1:1000 dilution; Cat. # ab220210; Abcam, Cambridge, UK), and anti-GFAP (1:1000 dilution; Cat. # ab4674; Abcam, Cambridge, UK). After incubation, the sections were rinsed with phosphate-buffered saline (PBS) and treated with an HRP-conjugated secondary antibody (EnVision kit, Dako, Copenhagen, Denmark) for 20 minutes. Staining was visualized using 3,3′-diaminobenzidine chromogen for 15 minutes, followed by hematoxylin counterstaining. Finally, the sections were examined under a light microscope by a blinded pathologist to ensure unbiased evaluation.

2.10 Morphometric Investigation

To quantify the immunoexpression of caspase-3, caspase-1, TNF-α, and GFAP in the cerebellum across the experimental groups, images were obtained from ten non-overlapping high-power fields (400× magnification) per section using a Leica ICC50W camera mounted on a Leica microscope. One section from each rat was analyzed, with ten rats included per group. The area percentage of positively stained brown immunoreactive cells was calculated from the digital images using ImageJ analysis software (version 1.47v; National Institutes of Health, Bethesda, MD, USA).

2.11 Quantitative Real-Time Reverse Transcription PCR (qRT-PCR)

Relative gene expression in cerebellar tissue was quantified using qRT-PCR. Approximately 100 mg of cerebellar tissue per sample was homogenized, and total RNA was extracted using Trizol reagent (Invitrogen, Life Sciences, Carlsbad, CA, USA). RNA concentration and purity (A260/A280 ≥1.8) were assessed using a NanoDrop spectrophotometer. Only RNA samples meeting the quality threshold were reverse transcribed into cDNA using a synthesis kit (Fermentas, Waltham, MA, USA). qRT-PCR was then conducted using SYBR Green (Bioline, myBio, Dublin, Ireland) Master Mix, gene-specific primers (Table 1), and *GAPDH* as the housekeeping gene for normalization. Gene expression levels were calculated using the $2^{-\Delta\Delta CT}$ method [45].

Table 1. The list of primer sequences of tested genes.

Gene	The nucleotide sequence (5′-3′)	Accession number
Nrf2	F: CCCATTGAGGGCTGTGATCT R: GCCTTCAGTGTGCTTCTGGTT	NM_031789.3
HO-1	F: GATGGCCTCCTTGTACCATATC R: AGCTCCTCAGGGAAGTAGAG	NM_012580.2
Bax	F: GGCGAATTGGCGATGAACTG R: ATGGTTCTGATCAGCTCGGG	NM_017059.2
Bcl-2	F: GATTGTGGCCTTCTTTGAGT R: ATAGTTCCACAAAGGCATCC	NM_016993.2
NF-κB	F: TGGGACGACACCTCTACACA R: GGAGCTCATCTCATAGTTGTCC	XM_006233360.5
GAPDH	F: TCAAGAAGGTGGTGAAGCAG R: AGGTGGAAGAATGGGAGTTG	NM_017008.4

Nrf2, Nuclear factor erythroid 2-related factor 2; HO-1, Heme oxygenase-1; Bax, Bcl-2-associated X protein; Bcl-2, B-cell lymphoma 2; NF-κB, Nuclear factor kappa-B; GAPDH, Glyceraldehyde-3-phosphate dehydrogenase.

2.12 Molecular Docking Analysis

Molecular docking was conducted to characterize the interaction profile of RA with Keap1, IKKβ, and caspase-3. The three-dimensional structure of RA was obtained from the PubChem database (https://pubchem.ncbi.nlm.nih.gov/) and prepared for docking analysis. Protein structures were retrieved from the PDB and processed through standard preparation steps, including removal of crystallographic water molecules and bound ligands, followed by the addition of hydrogen atoms. Docking simulations were performed using the SwissDock platform (http://www.swissdock.ch/), which utilizes the EADock DSS algorithm to predict optimal ligand–protein binding orientations and estimate binding free energies. All simulations were executed under default settings, and the most favorable poses were selected based on the lowest predicted ΔG values and cluster ranking. The resulting complexes were examined to identify key molecular interactions such as hydrogen bonding, hydrophobic contacts, and π-stacking between RA and amino acid residues within the active regions of Keap1, IKKβ, and caspase-3. Visualization and interaction mapping of the docking poses were carried out using Discovery Studio Visualizer (BIOVIA, San Diego, CA, USA).

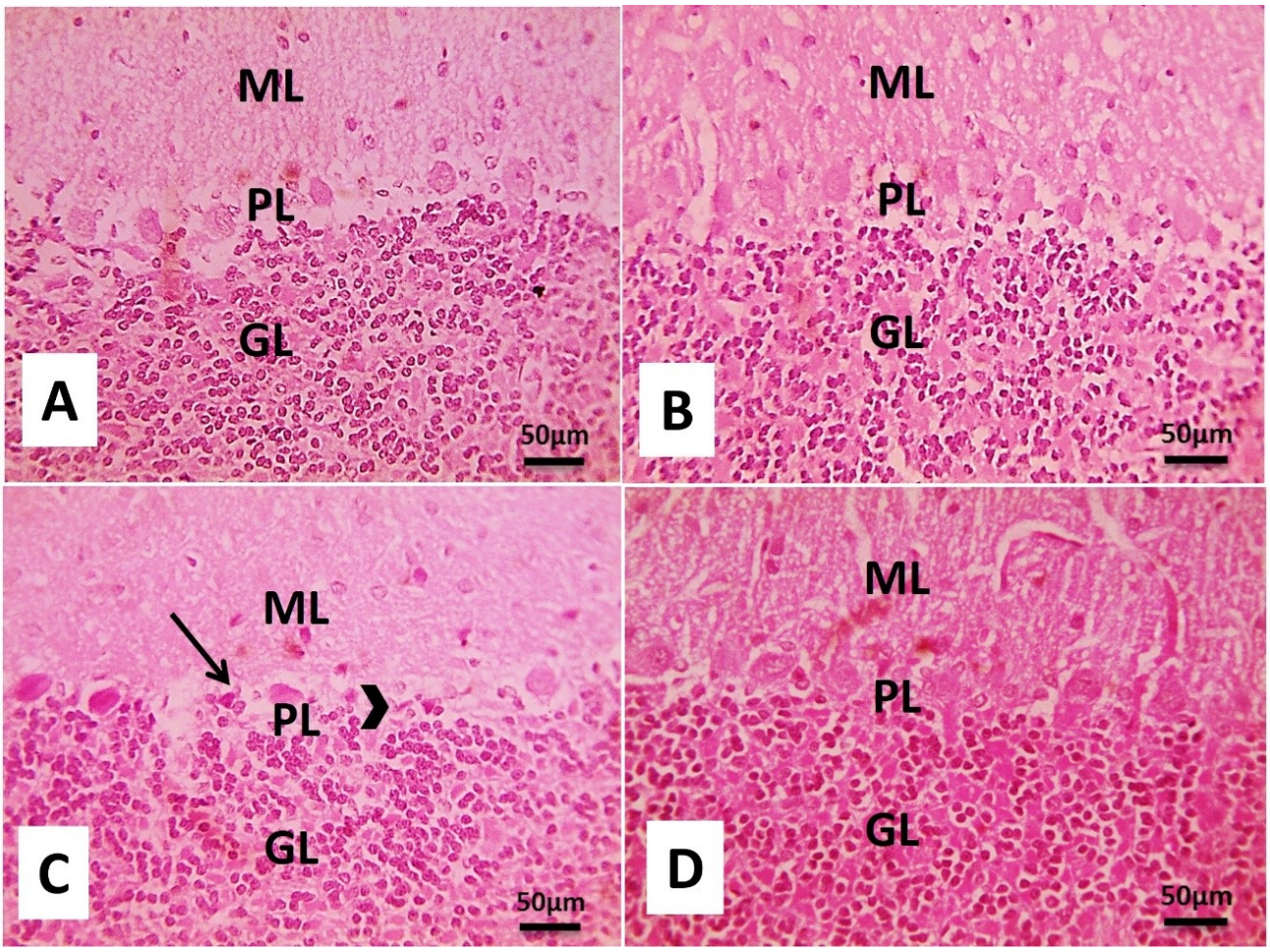


Fig. 1. Histological features of the cerebellar cortex in the experimental groups. Microscopic images showing nearly normal histological structures of the cerebellar cortex consisting of the molecular cell layer (ML), Purkinje cell layer (PL), and granule cell layer (GL) in the control (A) and RA (B) groups. Cerebellar sections from the GR group (C) show many shrunken, darkly stained, degenerated Purkinje cells with pyknotic nuclei (black arrow) and loss of Purkinje cells (arrowhead). Cerebellar sections from the GR+RA group (D) show a retained normal appearance of flask-shaped Purkinje neurons. H&E ×400, scale bar = 50 µm. RA, Rosmarinic acid; GR, Gamma radiation; H&E, hematoxylin and eosin.

2.13 Statistical Analysis

Statistical analyses were conducted using GraphPad Prism 8 (GraphPad Software, San Diego, CA, USA). Data were analyzed by one-way analysis of variance (ANOVA), followed by Tukey's post hoc test for multiple comparisons. Results are presented as mean ± standard deviation, and statistical significance was established at $p < 0.05$.

3. Results

3.1 Histology and Motor Function Recovery

To evaluate the extent of radiation-induced cerebellar tissue damage and assess the protective efficacy of RA, histological examination of H&E-stained sections revealed normal cerebellar architecture, with healthy Purkinje cells morphology in both the control (Fig. 1A) and RA (Fig. 1B) groups. In contrast, the GR group exhibited pronounced signs of Purkinje cell apoptosis, characterized by pyknotic nuclei and subsequent cellular degeneration (Fig. 1C). Remarkably, rats in the GR group treated with RA demonstrated substantial restoration of Purkinje cell morphology (Fig. 1D). These findings highlighted the protective effect of RA on cerebellar cytoarchitecture in rats exposed to GR.

To evaluate the impact of GR exposure and RA treatment on motor function, the rotarod test was employed to assess cerebellar-dependent motor coordination and balance. A one-way ANOVA revealed a highly significant effect of treatment on the latency to fall ($F(3, 36) = 276.2$, $p < 0.0001$). Compared with the control group, GR-intoxicated rats exhibited a substantial and significant reduction in retention time on the rotating rod by 63.1% ($p < 0.0001$), indicating severe motor impairment. Conversely, RA treatment of GR-exposed animals (GR+RA group) produced a marked improvement in motor performance, with retention time increasing by 126.7% relative to the GR group ($p < 0.0001$). The RA-only group did not differ significantly

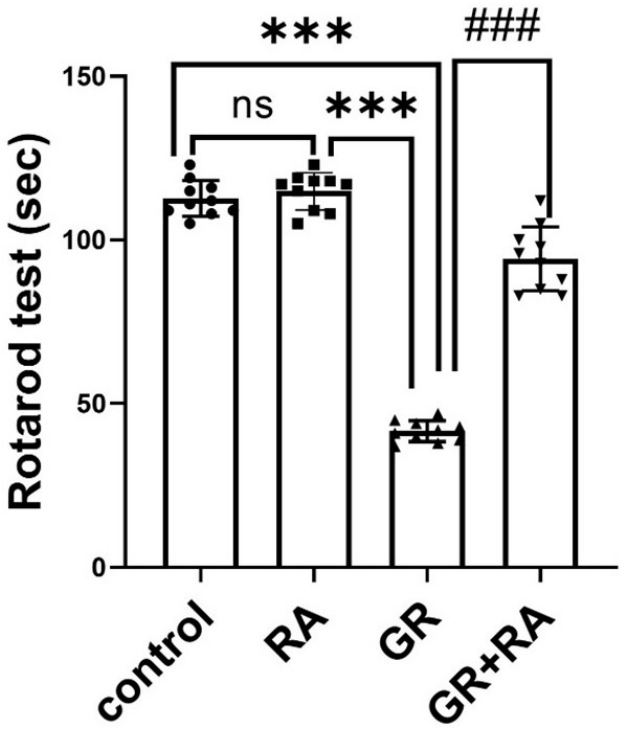


Fig. 2. Effect of RA on motor performance assessed by the rotarod test. Data are expressed as mean ± standard deviation (SD). Statistical significance was determined using one-way ANOVA coupled with Tukey's post hoc test for multiple pairwise comparisons. $^{***}p < 0.001$ indicates a significant difference relative to the control group; $^{###}p < 0.001$ denotes a significant difference relative to the GR-treated group. ns, not significant. n = 10 rats per group. ANOVA, Analysis of variance.

from the control group ($p = 0.8728$), suggesting that RA alone does not adversely affect baseline motor coordination. Notably, the GR+RA group still demonstrated a significantly lower retention time compared with the control group by 16.3% ($p < 0.0001$), indicating partial but substantial recovery of motor function (Fig. 2). These findings demonstrate that RA administration effectively ameliorates GR-induced motor deficits, likely through the preservation of cerebellar neuronal integrity and function.

3.2 RA Alleviates Oxidative Stress via Nrf2/HO-1

To elucidate the mechanisms underlying GR-induced cerebellar toxicity, oxidative stress markers were evaluated in cerebellar supernatant alongside the gene expression levels of *Nrf2* and *HO-1*. The GR group exhibited a pronounced increase in MDA concentration ($F(3, 36) = 921.7$, $p < 0.0001$) by 1341.9%, coupled with significant reductions in SOD activity ($F(3, 36) = 426.4$, $p < 0.0001$) by 83.1%, CAT activity ($F(3, 36) = 529.1$, $p < 0.0001$) by 92.5%, and GSH content ($F(3, 36) = 384.1$, $p < 0.0001$) by 91.1% compared with the control group. Administration of RA to GR-exposed rats markedly decreased MDA levels by 68.6% while increasing SOD activity, CAT activity, and GSH content by 214.8%, 636.3%, and 454.7%, respectively (Fig. 3A–D). The reductions in SOD and CAT activities in the GR group corresponded with a significant downregulation of *Nrf2* ($F(3, 36) = 101.1$, $p < 0.0001$) and *HO-1* ($F(3, 36) = 174.5$, $p < 0.0001$) mRNA expression by 86.6% and 92.9%, respectively, relative to controls. In contrast, the GR+RA group displayed a marked upregulation of *Nrf2* and *HO-1* by 374.3% and 626.9%, respectively (Fig. 3E,F). These results indicated that the elevation of endogenous cerebellar antioxidant enzyme levels in GR-exposed rats is primarily mediated by the RA-induced activation of the *Nrf2*/*HO-1* signaling pathway. Molecular docking analysis revealed that RA exhibited favorable binding to Keap1 with a binding energy of −6.849 kcal/mol, establishing multiple interactions with key residues including Arg470, Asn469, His516, Cys518, and Gln563 (Table 2). The interaction with Cys518, a critical residue for Keap1-Nrf2 complex stabilization, suggests that RA may competitively bind to Keap1, thereby disrupting the Keap1-Nrf2 interaction and facilitating Nrf2 nuclear translocation. This computational finding provides structural evidence supporting the observed upregulation of Nrf2/HO-1 pathway and subsequent enhancement of antioxidant defenses.

3.3 RA Suppresses NF-κB-Mediated Neuroinflammation and NLRP3-Dependent Pyroptosis

To assess the inflammatory response to GR and evaluate the anti-inflammatory potential of RA, the expression of NF-κB and its downstream inflammatory mediators was examined. Exposure to GR resulted in pronounced cerebellar inflammation, as indicated by a significant upregulation of *NF-κB* gene expression ($F(3, 36) = 610.6$, $p < 0.0001$), which increased by 571.3%. This was accompanied by substantial elevations in pro-inflammatory cytokines, including TNF-α immunoexpression ($F(3, 36) = 244.4$, $p < 0.0001$) by 1175.9%, IL-1β protein levels ($F(3, 36) = 281.1$, $p < 0.0001$) by 405.6%, and IL-6 ($F(3, 36) = 257.7$, $p < 0.0001$) by 545.5% compared with the control group. Furthermore, immunoexpression of GFAP-positive astrocytes ($F(3, 36) = 26.79$, $p < 0.0001$) showed a 71.2% increase relative to the control group. Remarkably, treatment with RA in GR-exposed rats (Group IV) significantly mitigated cerebellar inflammation, resulting in decreases in NF-κB, TNF-α, IL-1β, IL-6, and GFAP expression levels by 40.1%, 90.0%, 41.8%, 42.1%, and 34.1%, respectively, compared with the GR group (Fig. 4A–H; Fig. 5A–E). These findings clearly demonstrated that RA confers a strong anti-inflammatory effect, effectively suppressing GR-induced cerebellar inflammation. The anti-inflammatory mechanism was further supported by molecular docking analysis, which demonstrated robust binding of RA to IKKβ with a binding energy of −7.194 kcal/mol. RA established six hydrogen bonds and multiple hydrophobic interactions with key residues including Gln611, Leu547, Ser550, Ala453, and Ile608 within the IKKβ active site (Ta-

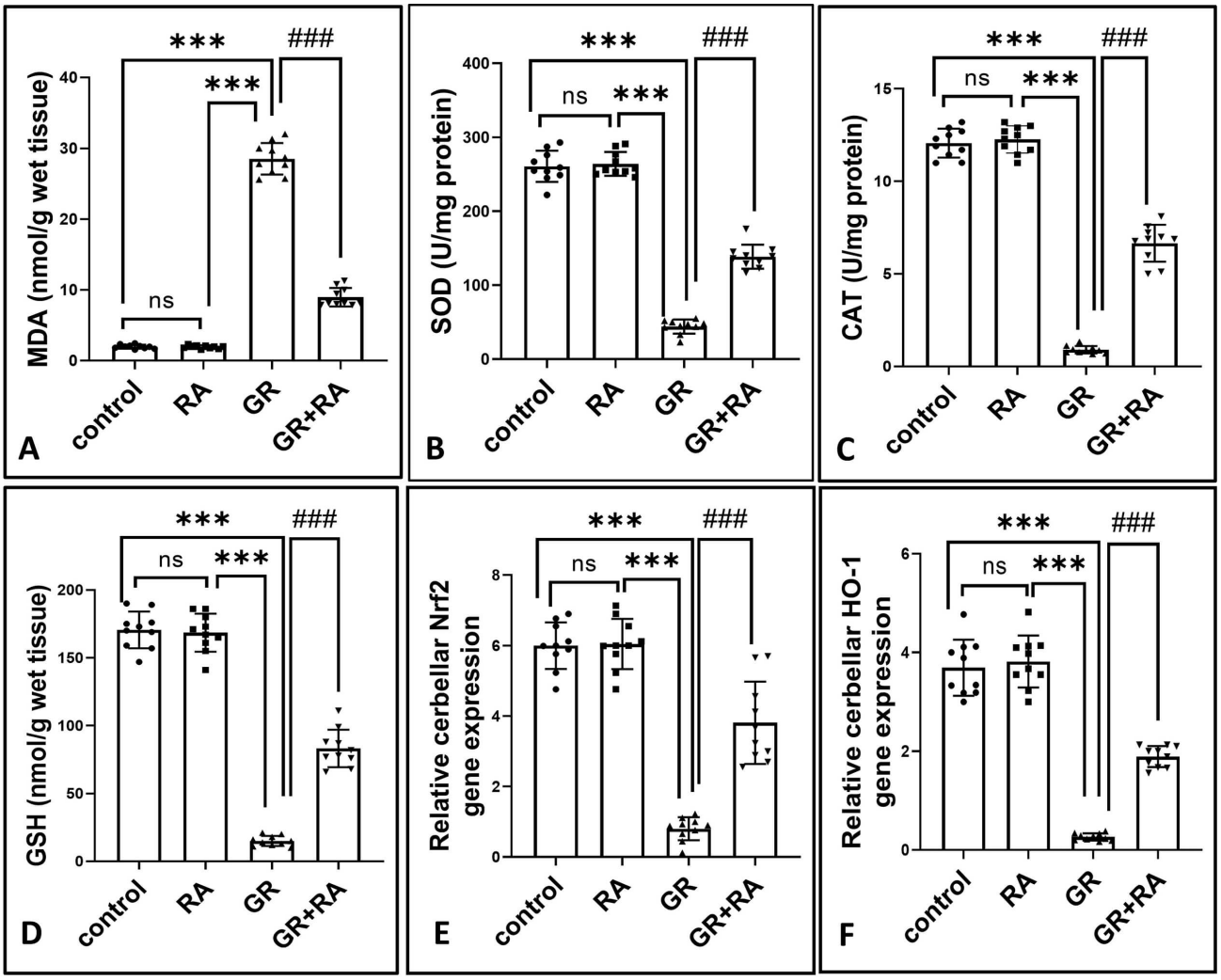


Fig. 3. Effect of RA on oxidative stress markers and *Nrf2*/*HO-1* gene expression in cerebellar tissues. (A) MDA content, (B) SOD activity, (C) CAT activity, and (D) GSH content in the control, RA, GR, and GR+RA groups. (E,F) Relative gene expression of *Nrf2* and *HO-1*. MDA and GSH contents are expressed as nmol/g wet tissue, whereas SOD and CAT activities are expressed as U/mg protein. Data are expressed as mean ± SD. $^{***}p < 0.001$ significant from the control group; $^{###}p < 0.001$ significant from the GR group using one-way ANOVA followed by Tukey post hoc test to compare all means. ns, not significant. n = 10 rats per group. MDA, Malondialdehyde; SOD, Superoxide dismutase; CAT, Catalase; GSH, Glutathione.

Table 2. Binding affinities and molecular interaction profiles of RA with Keap1, IKKβ, and caspase-3, including hydrogen bonds, hydrophobic contacts, and π-stacking interactions.

Protein	Binding affinity (ΔG, kcal/mol)	Key residues interacting	Hydrogen bonds	Hydrophobic interactions	π-stacking
Keap1	–6.849	Cys518, His516, Arg470, Asn469, Gln563	5	Leu135, Val467, Val561, Val608	YES
IKKβ	–7.194	Gln611, Leu547, Val46, Ser550, Ala453, Ile608, Arg452	6	Leu547, Arg452	No
Caspase-3	–7.550	Gly165, Phe256, Thr255, Arg164, Thr62, Met61, Tyr204, Cys220	7	Val266, Ser205, Ile206, Tyr203	YES

Abbreviations: ΔG, binding free energy (kcal/mol); Keap1, Kelch-like ECH-associated protein; IKKβ, inhibitor of nuclear factor kappa-B kinase subunit beta; H-bonds, hydrogen bonds; π-stacking, pi–pi stacking interactions. Lower (more negative) ΔG values indicate stronger predicted binding affinity.

ble 2). This interaction pattern suggests that RA may inhibit IKKβ kinase activity, thereby preventing IκB phosphorylation and subsequent NF-κB nuclear translocation. The docking results provide a molecular rationale for the observed suppression of NF-κB gene expression and reduction in pro-inflammatory cytokine levels.

To investigate the influence of RA on GR-induced pyroptosis, cerebellar protein levels of NLRP3 and the pro-inflammatory cytokines IL-1β and IL-18, which are cleaved by caspase-1, along with the immunoexpression of caspase-1, were evaluated.GR exposure led to a significant elevation in cerebellar pyroptotic markers, with NLRP3 (F (3, 36) = 753.7, $p < 0.0001$) increasing by 1294.7%, IL-18 (F (3, 36) = 165.7, $p < 0.0001$) by 301.7%, and caspase-1 immunoexpression (F (3, 36) = 75.67, $p < 0.0001$) by 584.2% compared with the control group (Fig. 6A–H). IL-1β levels, which are shared with the inflammatory response, were elevated as described in Section 3.3 (Fig. 4G). Conversely, RA treatment in GR-exposed rats markedly attenuated these elevations, reducing NLRP3, caspase-1, IL-1β, and IL-18 levels by 69.4%, 75.4%, 41.8%, and 46.1%, respectively, relative to the GR group. These results confirmed that RA effectively inhibits GR-induced pyroptosis, primarily by suppressing the NLRP3/caspase-1/IL-1β signaling pathway. The inhibition of pyroptosis is mechanistically linked to RA's dual effects on upstream inflammatory signaling: (1) suppression of NF-κB activation through IKKβ inhibition as demonstrated by molecular docking, which reduces NLRP3 inflammasome priming, and (2) direct antioxidant activity through Nrf2 activation, which limits ROS-mediated NLRP3 activation.

3.4 RA Inhibits Neuronal Apoptosis

To evaluate the impact of RA on radiation-induced apoptotic cell death in the cerebellum, the expression of apoptotic markers was assessed. GR exposure resulted in a significant increase in caspase-3 immunoexpression (F (3, 36) = 192.7, $p < 0.0001$) by 1135.3%, along with a pronounced elevation in *Bax* mRNA expression (F (3, 36) = 304, $p < 0.0001$) by 252%. Conversely, *Bcl-2* gene expression (F (3, 36) = 128.0, $p < 0.0001$) decreased by 58.2% relative to control rats (Fig. 7A–C,E–G). Administration of RA in conjunction with GR significantly reduced caspase-3 and *Bax* levels by 81.9% and 50.8%, respectively, while markedly upregulating the anti-apoptotic *Bcl-2* expression by 68.8% compared with the GR group (Fig. 7D,E–G). These results demonstrated that RA exerts potent anti-apoptotic effects in Purkinje cells of GR-exposed rats, which accounts for the notable morphological restoration observed in Group IV. Molecular docking analysis revealed the strongest binding interaction of RA with caspase-3, exhibiting a binding energy of −7.550 kcal/mol (Table 2). RA established seven hydrogen bonds and multiple hydrophobic contacts with critical residues including Gly165, Thr255, Arg164, Thr62, Met61, Tyr204, and Cys220 within the caspase-3 active site. The interaction with Cys220, a residue essential for caspase-3 catalytic activity, suggests that RA may directly inhibit caspase-3 enzymatic function. The π-stacking interactions observed with Tyr203 and Tyr204 further stabilize the RA-caspase-3 complex. This computational finding provides strong mechanistic evidence for the observed reduction in caspase-3 immunoexpression and the overall anti-apoptotic effect of RA in cerebellar tissues.

3.5 Molecular Docking Verification of Target Binding

Molecular docking analysis revealed that RA binds favorably to Keap1, IKKβ, and caspase-3, with binding energies of −6.849, −7.194, and −7.550 kcal/mol, respectively. Among the evaluated targets, caspase-3 exhibited the strongest affinity, followed by IKKβ and Keap1. The compound formed several stabilizing hydrogen bonds and hydrophobic contacts with critical amino acid residues within the active sites of these proteins. In Keap1, interactions with Arg470, Asn469, His516, Cys518, and Gln563 suggest that RA may interfere with Keap1–Nrf2 binding, thereby facilitating Nrf2 activation and enhancing antioxidant defense. Its favorable docking with IKKβ supports a potential inhibitory influence on NF-κB signaling and subsequent inflammatory responses. Additionally, the strong interaction with caspase-3 indicates a possible regulatory effect on apoptotic pathways. Collectively, these docking results provide mechanistic support for the antioxidant, anti-inflammatory, and anti-apoptotic properties of RA (Table 2 and Fig. 8).

4. Discussion

Radiation therapy has long been a cornerstone in the management of malignancies; however, its unavoidable effects on adjacent healthy tissues, leading to toxicity, remain a major clinical challenge. Despite substantial research into potential interventions for GR-induced neurotoxicity, the precise underlying mechanisms have not been fully elucidated. A clearer understanding of the involvement of neuroproteins in GR is essential to enhance survival outcomes for patients undergoing RT. To the best of our knowledge, this study represents the first investigation into the neuroprotective effects of RA on GR-induced cerebellar damage, coupled with an in-depth exploration of its mechanistic actions supported by molecular docking analysis.

Oxidative stress induced by IR primarily results from the excessive generation of ROS, which deplete endogenous antioxidant defenses and damage intracellular macromolecules such as DNA, proteins, and lipids [46,47]. In this study, a single 6 Gy dose of GR significantly increased cerebellar MDA levels while markedly reducing SOD and CAT activities and GSH content in cerebellar supernatant, consistent with previous reports [46,48]. The heightened oxidative stress in cerebellar tissue can be attributed to intracellular water radiolysis generating FRs, and the high PUFA

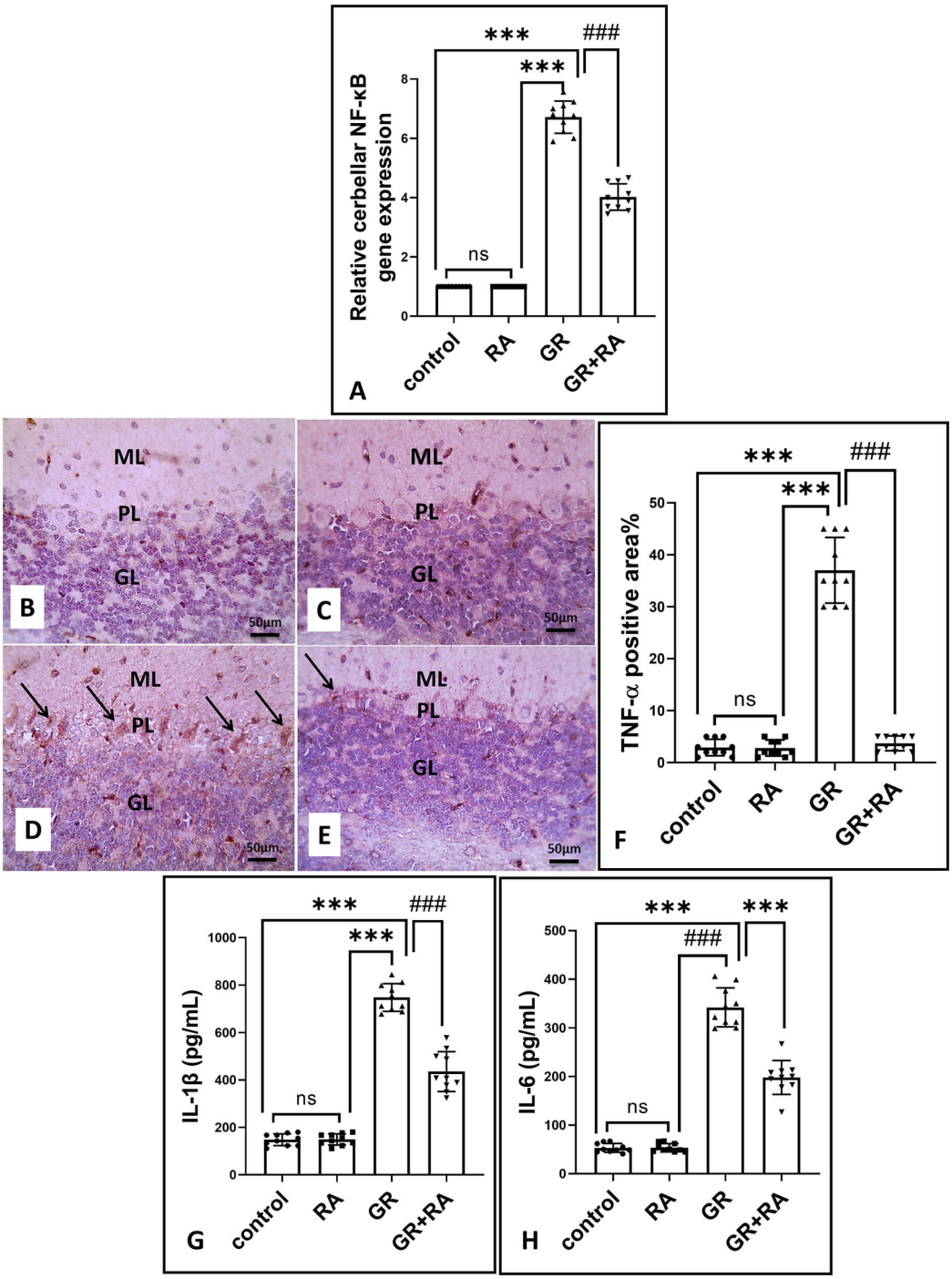


Fig. 4. Anti-inflammatory effect of RA on GR-induced cerebellar inflammation. (A) mRNA of *NF-κB*. Microscopically immunostained cerebellar sections against TNF-α show negatively stained Purkinje neurons in the control (B) and RA (C) groups n = 10 rats. Cerebellar sections from the GR group n = 10 rats. (D) show many positively brown-stained Purkinje neurons (thin black arrows). Cerebellar sections from the GR+RA group n = 10 rats. (E) show negatively stained Purkinje neurons (thin black arrow). High magnification ×400, scale bar = 50 µm. (F) Bars demonstrate TNF-α positive area (%). (G,H) ELISA levels of IL-1β and IL-6. Values are represented as mean ± SD. $^{***}p < 0.001$ vs. control group; $^{###}p < 0.001$ vs. GR group using one-way ANOVA followed by Tukey post hoc test to compare all means. ns, not significant. TNF-α, Tumor necrosis factor-alpha; ELISA, Enzyme-linked immunosorbent assay.

content of axonal myelin sheaths, which renders neurons highly susceptible to lipid peroxidation [16,49,50]. Conversely, combined GR and RA treatment markedly reduced MDA levels, restored SOD and CAT activities, and increased GSH content. These findings align with Karaca et al. [51], who demonstrated RA's suppression of oxidative stress in cerebral and hippocampal regions. The antioxidant efficacy of RA arises from its inhibition of PUFA oxi-

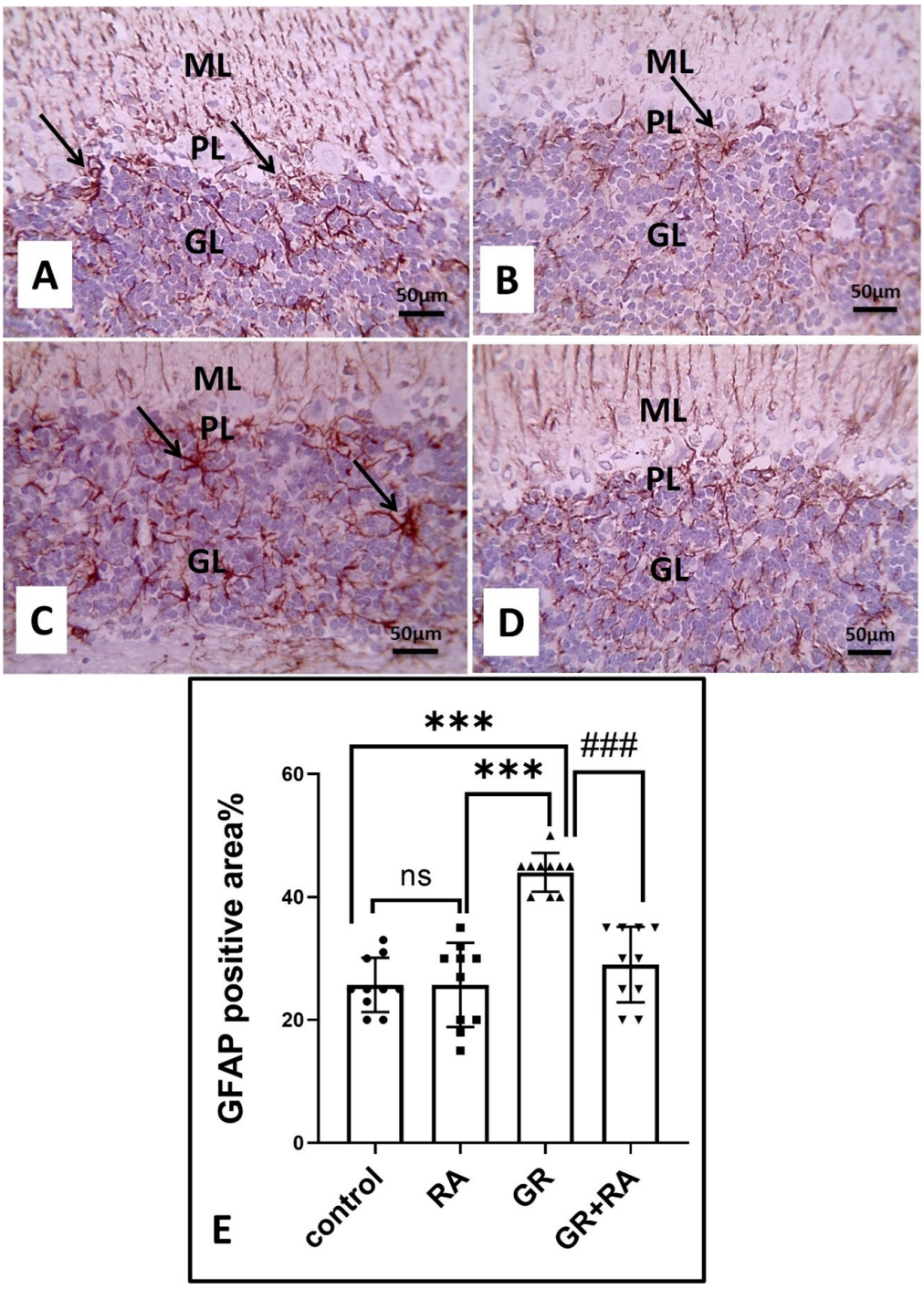


Fig. 5. Effect of RA on GFAP-positive astrocyte activation in cerebellar cortex. (A,B) Microscopic analysis of immunostained cerebellar cortex sections revealing normally, positively brown-stained astrocytes for GFAP (black arrows) in control and RA groups n = 10 rats. (C) The number of positively stained astrocytes for GFAP (black arrows) increased with more and thicker branches in the GR group n = 10 rats. (D) The number decreased in the GR+RA group n = 10 rats compared with the GR group. High magnification ×400, scale bar = 50 µm. (E) Bars demonstrate the mean ± SD of *GFAP*-positive area% in cerebellar cortex. $^{***}p < 0.001$ against control group; $^{###}p < 0.001$ against GR group using one-way ANOVA followed by Tukey post hoc test. ns, not significant.

dation in cell membranes, thereby protecting neuronal cells from lipid peroxidation [52], and its ability to chelate transition metals, such as iron and copper, thereby preventing FR catalysis [53].

The Nrf2/HO-1 pathway is a well-known endogenous intracellular system that responds to environmental stress by modulating antioxidant defenses, making it a critical target for treating diseases associated with oxidative dam-

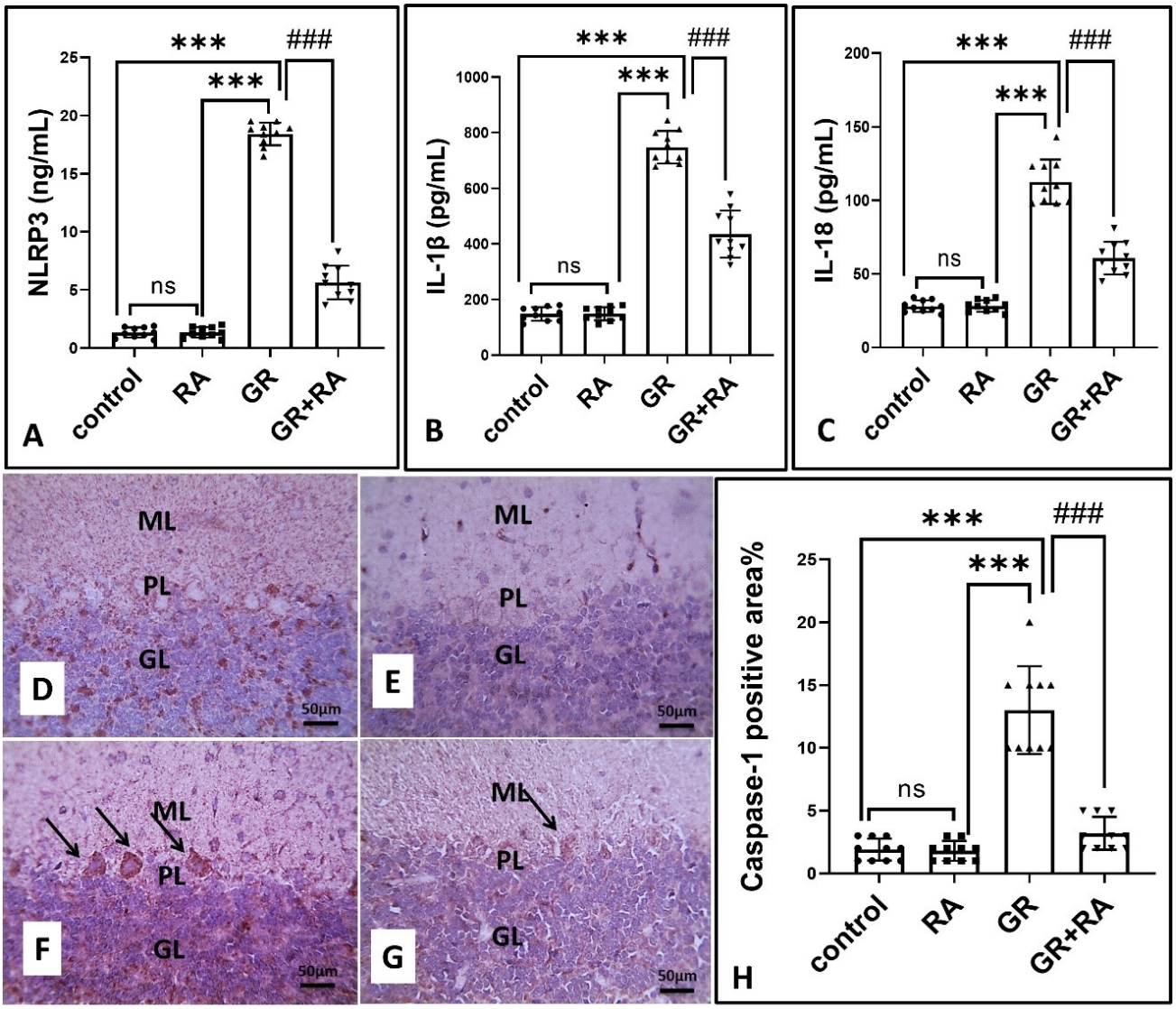


Fig. 6. Effect of RA on protein levels of pyroptotic markers. (A) NLRP3, (B) IL-1β, and (C) IL-18. Microscopic images of immunostained sections show negatively stained neurons for caspase-1 in the control and RA groups n = 10 rats (D,E). The GR group n = 10 rats (F) shows an increase in positively brown-stained neurons (black arrows). The GR+RA group n = 10 rats (G) shows a decrease in positively stained neurons. (H) Bars show caspase-1 positive area (%) in cerebellar cortex. ×400, scale bar = 50 μm. Data as mean ± SD. $^{***}p < 0.001$ against control; $^{###}p < 0.001$ against GR group. ns, not significant. NLRP3, NLR family pyrin domain-containing 3; IL-1β, Interleukin-1 beta; IL-18, Interleukin-18.

age [54]. Based on previous data, our findings indicated that GR significantly suppressed the gene expression of the *Nrf2*/*HO-1* pathway, leading to the downregulation of antioxidant enzyme transcription. These results align with the study by Zhang et al. [55], which reported that radiation exposure reduces both protein levels and gene expression of the *Nrf2* pathway. Conversely, the combination of RA with GR upregulated the mRNA expression of the *Nrf2*/*HO-1* cascade, explaining its role in enhancing antioxidant activity. This observation is consistent with the findings of Cui et al. [56], who documented the neuroprotective effects of RA in a mouse model of ischemic stroke-induced oxidative stress, demonstrating its ability to elevate both gene expression and protein levels. The positive impact of RA can be attributed to its interaction with *Keap1*, which facilitates the release of *Nrf2*. Once freed, *Nrf2* translocates into the nucleus, where it binds to AREs, triggering the transcription of cytoprotective genes [57]. NF-κB is a well-known inflammatory transcription factor that plays a pivotal role in the cellular response to IR. Furthermore, IR damages cellular DNA, leading to the formation of ROS, which stimulates various intracellular signaling cascades [58]. Additionally, several studies have reported that IR activates NF-κB [59,60].

In resting states, NF-κB remains bound to IκB in the cytoplasm. Upon stimulation, the phosphorylation of IKK

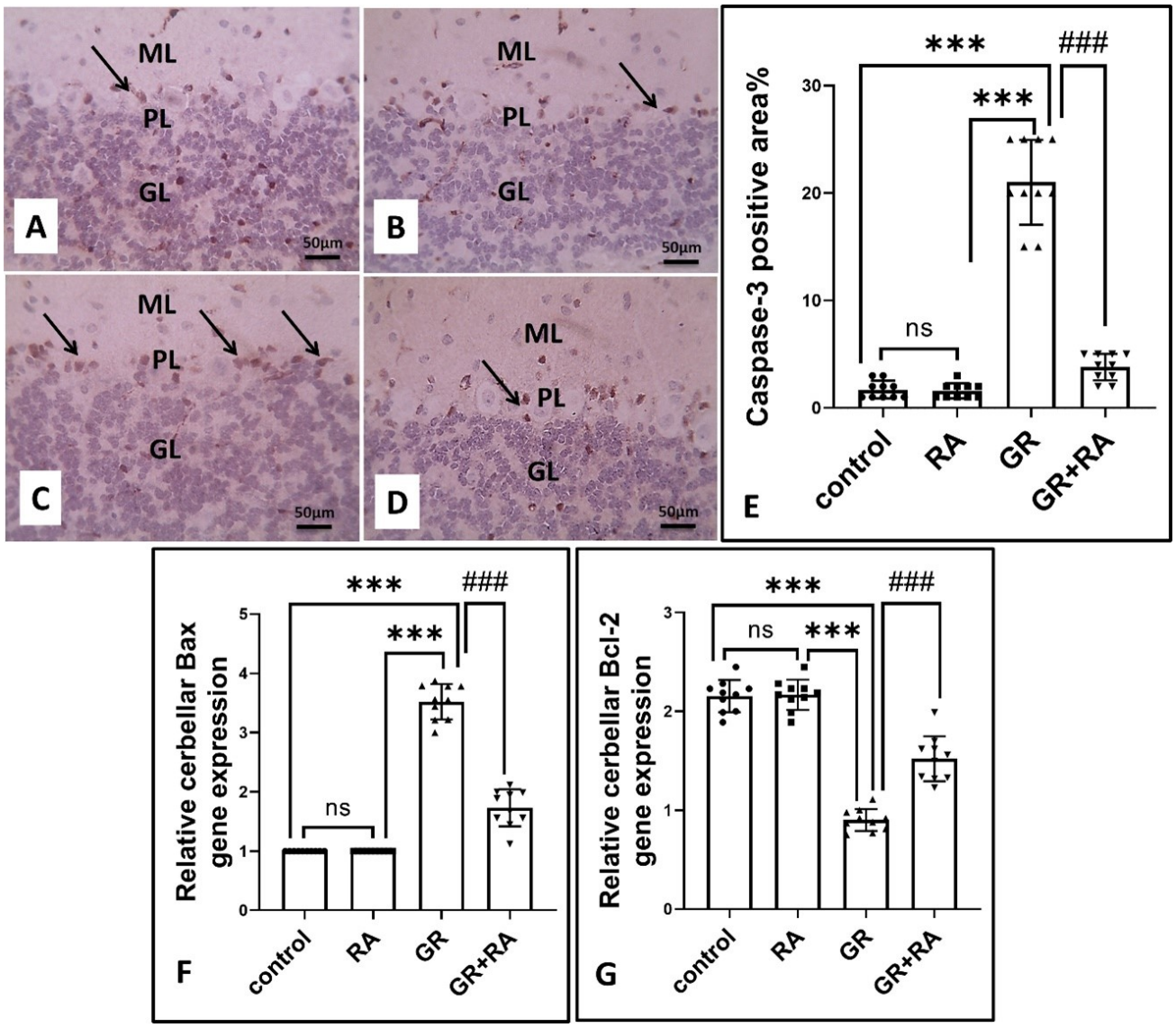


Fig. 7. Effect of RA on apoptotic markers in cerebellar tissues. Microscopic immunostained cerebellar sections against caspase-3 show negatively stained Purkinje neurons in control n = 10 rats (A) and RA n = 10 rats (B) groups. The GR group n = 10 rats (C) exhibits numerous positively brown-stained Purkinje neurons (indicated by the thin black arrow). The GR+RA group n = 10 rats (D) shows markedly decreased staining. (E) Bars show caspase-3 positive area (%). High magnification ×400, scale bar = 50 μm. (F,G) Relative gene expression of *Bax* and *Bcl-2*. Values are mean ± SD. $^{***}p < 0.001$ against control group; $^{###}p < 0.001$ against GR group. ns, not significant.

induces IκB degradation, leading to its dissociation from NF-κB. This enables NF-κB to translocate into the nucleus, where it initiates the transcription of genes responsible for producing pro-inflammatory cytokines [61]. In addition, irradiation promotes FR generation, further driving the production of IL-1β and TNF-α [62,63]. Astrocytes, a type of glial cell, play a vital role in immune responses within the brain, especially following pathological injury. Activated astrocytes release substantial amounts of inflammatory cytokines, which may contribute to neuronal death [64,65]. Our findings showed that GR significantly increases NF-κB expression, elevates cerebellar TNF-α, IL-6, and IL-1β protein levels, and increases the number of GFAP-immunostained activated astrocytes. These results align with those of Wang et al. [66], who reported GR-induced upregulation of cerebral NF-κB protein levels, and Khateeb [36], who demonstrated that radiation in female rats induced ovarian injury through inflammation, characterized by elevated IL-1β and TNF-α. Besides, they align with He et al. [67], who showed an increased number of GFAP-positive cells in the thalamus following GR. Notably, combined RA treatment in our study exerted potent anti-inflammatory effects in cerebellar tissue by reducing *NF-κB* gene expression, lowering cytokine levels, and

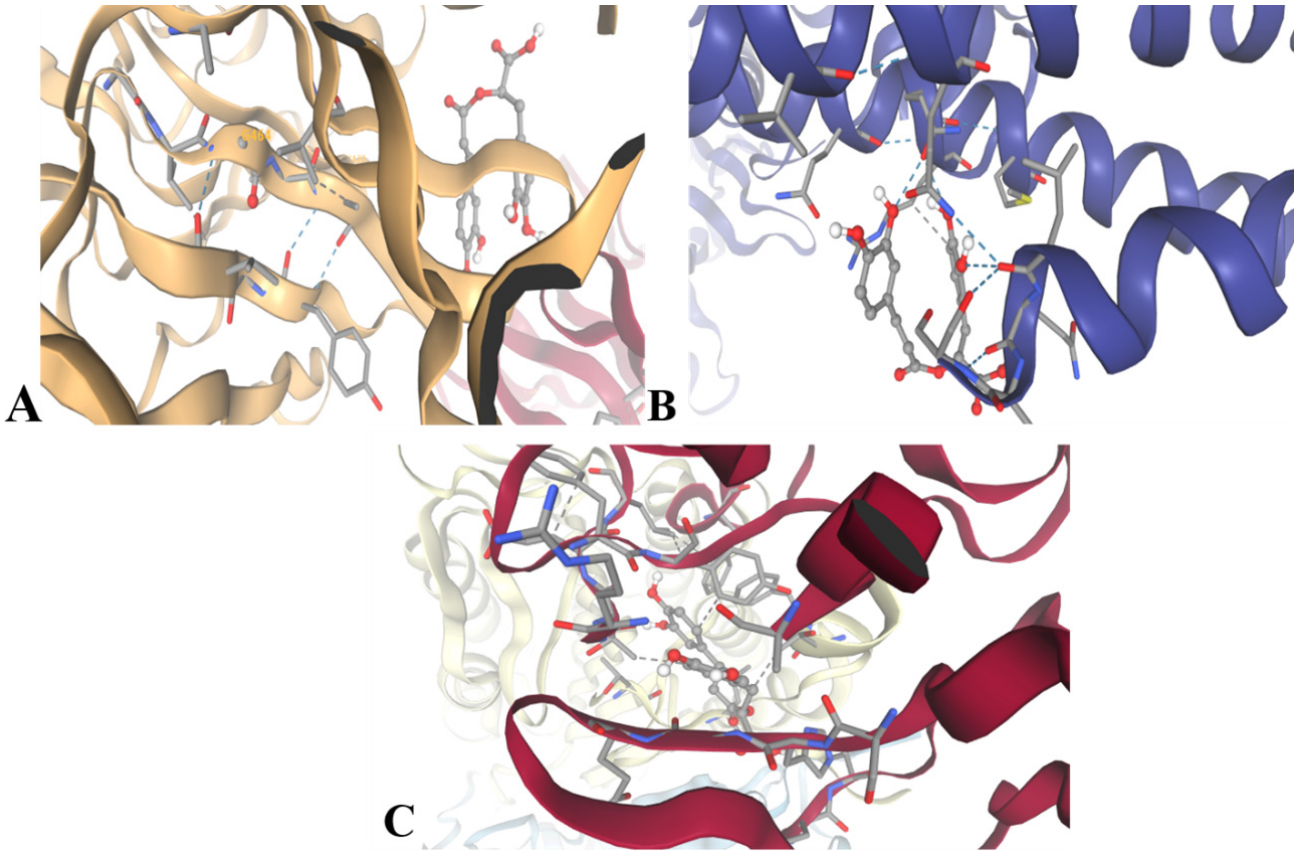


Fig. 8. Molecular docking analysis of RA with key proteins involved in oxidative stress, inflammation, and apoptosis pathways. (A) Binding interaction of RA with Keap1. (B) Binding interaction of RA with IKKβ. (C) Binding interaction of RA with caspase-3. The figures illustrate the binding mode of RA within the active site of each target protein and the associated hydrogen bonds, hydrophobic contacts, and π-stacking interactions with key amino acid residues.

markedly decreasing *GFAP* expression, thereby diminishing the number of activated astrocytes. This finding aligns with that of Karaca et al. [51], who discovered that RA mitigates tramadol-induced neurotoxicity by suppressing hippocampal inflammation through the inhibition of *NF-κB*, *TNF-α*, *IL-1β*, and *GFAP* expression.

Multiple mechanisms can explain the inhibitory effect of RA on the *NF-κB* pathway. First, its scavenging effect on ROS prevents *NF-κB* activation. Additionally, previous studies have reported that RA suppresses IKK-β activity, a key regulator of the *NF-κB* signaling pathway [68]. Furthermore, RA may exert anti-inflammatory effects through its upregulation of *Nrf2*, as research indicates that *Nrf2* depletion exacerbates *NF-κB*-mediated inflammatory responses, while RA stimulates *Nrf2* expression [69]. Gamma radiation plays a significant role in inducing neuronal pyroptosis, a form of programmed cell death associated with inflammation. Exposure to GR leads to DNA damage and oxidative stress, triggering the activation of inflammasomes, particularly the *NLRP3* inflammasome, in neuronal cells. This activation results in the cleavage of *caspase-1*, which subsequently processes pro-inflammatory cytokines such as *IL-1β* and *IL-18*, amplifying neuroinflammation. Our study revealed that exposure of rats to GR increases the protein level of *NLRP3* inflammasomes, along with enhanced immunostaining of *caspase-1*, and a marked increase in *IL-1β* and *IL-18* levels. These findings coincide with the results reported by Smith et al. [70]. Interestingly, RA mitigates neuronal pyroptosis by reversing these pyroptotic changes, supporting previous work by Karaca et al. [51], who documented the downregulatory effect of RA on *NLRP3* mRNA expression in cerebral and hippocampal tissues of rats treated with tramadol. The inhibitory effect of RA on *NLRP3* can be attributed to its potent antioxidant properties, which reduce ROS formation, a key factor in inflammasome activation.

Furthermore, RA suppresses *NF-κB* activation, a crucial regulator of inflammasome response, further contributing to its neuroprotective effects against radiation-induced neuronal pyroptosis. Radiation appears to initiate an apoptotic program through the generation of ROS, which can activate the mitochondrial pathway and lead to the release of caspase-activating factors. Consequently, oxidative stress plays a direct role in radiation-induced apoptosis [71].

In this study, increased levels of *caspase-3* and *Bax*, accompanied by decreased *Bcl-2* expression, were ob-

served, with histological examinations confirming a rise in apoptotic Purkinje cells. In contrast, the administration of RA to GR-exposed rats significantly reduced neuronal apoptosis markers, consistent with findings from Karaca et al. [51] and Lee et al. [32]. Furthermore, RA treatment improved cerebellar morphology, maintaining the structural integrity of Purkinje cells, thereby underscoring its potent neuroprotective effects. The functional relevance of these molecular and histopathological findings was corroborated through rotarod behavioral assessment. The cerebellum plays an indispensable role in coordinating voluntary movements, maintaining postural equilibrium, and facilitating motor learning, with Purkinje cells serving as the principal output neurons integrating synaptic inputs to regulate fine motor coordination. The present study employed a post-irradiation administration protocol, wherein RA was initiated immediately following GR exposure and continued for 14 days. This therapeutic paradigm was selected to evaluate the capacity of RA to mitigate already-established radiation injury, reflecting the clinical scenario where patients receive RT prior to intervention for radiation-induced toxicity. While we acknowledge that pre-radiation administration might confer additional cytoprotection through enhanced baseline antioxidant status, the post-treatment regimen addresses the more clinically relevant question of whether RA can attenuate the progressive inflammatory and degenerative cascades that follow radiation exposure. Future comparative studies examining pre- versus post-irradiation administration schedules would be valuable to identify the optimal therapeutic window for RA-mediated neuroprotection. When compared with amifostine, the only FDA-approved radioprotector, RA offers several advantages including oral bioavailability, ability to cross the BBB, established safety profile from centuries of dietary use, and cost-effective accessibility from natural sources, whereas amifostine requires intravenous administration and is associated with significant toxicities including hypotension, nausea, and hypocalcemia [72,73]. However, amifostine has well-established clinical protocols, whereas RA requires further preclinical and clinical evaluation to define optimal dosing and efficacy [74].

Limitations

Despite the promising findings, several limitations warrant consideration. First, this investigation utilized a single dose of RA (120 mg/kg) without conducting a dose-gradient experiment to confirm the optimal therapeutic concentration. While the selected dose was based on previous neuroprotective studies [35], the absence of dose-response data precludes determination of the minimum effective dose and the potential for dose-dependent efficacy. Future studies incorporating multiple RA concentrations would be valuable to establish the optimal therapeutic window and dose-response relationship. Second, this investigation utilized a single acute radiation dose (6 Gy), which does not replicate the fractionated irradiation regimens employed in clinical RT, thereby limiting direct extrapolation to patient settings. Third, the study was confined to male rats, precluding assessment of potential sex-specific differences in radiation sensitivity or RA responsiveness. Fourth, the present study was conducted exclusively using an *in vivo* animal model and lacks *in vitro* neuronal cell verification. While our findings demonstrate neuroprotective effects in cerebellar tissue, we cannot exclude the possibility that RA's protective effects are mediated indirectly through peripheral tissues or systemic factors rather than through direct action on cerebellar neurons. Future studies employing primary cerebellar neuron cultures or neuronal cell lines would help confirm the direct neuroprotective effects of RA at the cellular level. Fifth, although molecular docking predicted favorable binding of RA to Keap1, IKKβ, and caspase-3, and our biochemical data support involvement of the Nrf2/HO-1 and NF-κB/NLRP3 pathways, we did not perform knockout or inhibitor intervention experiments to definitively establish the absolute dependence of RA's protective effects on Nrf2 activation. Without genetic or pharmacological manipulation of these pathways, we cannot conclusively attribute the observed protection solely to Nrf2-mediated mechanisms. Future studies employing Nrf2 knockout animals or specific pathway inhibitors would provide definitive confirmation of the causal role of these signaling cascades in RA-mediated neuroprotection. Sixth, while our study provides valuable evidence through ELISA and IHC, we acknowledge that Western blot analysis for NF-κB, NLRP3, and caspase-3 proteins, as well as nuclear-cytoplasmic fractionation combined with immunofluorescence staining for Nrf2 activation status, would have provided more definitive mechanistic confirmation. However, due to limitations in laboratory facilities and equipment availability, these experiments could not be performed in the present study. We explicitly acknowledge that incorporating Western blotting, EMSA, immunofluorescence, or nuclear–cytoplasmic fractionation would have strengthened the mechanistic validation of NF-κB, NLRP3, and caspase-3 activation, and we identify these assays as essential components of future work. Additionally, we acknowledge that cell-based assays and gene-knockdown experiments would provide stronger genetic evidence to further validate the involvement of Nrf2/HO-1 and NF-κB/NLRP3 pathways. However, without specific knockout or inhibitor intervention experiments, we cannot definitively establish the absolute dependence of RA's protective effects on Nrf2 activation. Furthermore, the clinical applicability of RA is constrained by its oral bioavailability, blood-brain barrier permeability, and the need for dose conversion from animal to human, as well as challenges common to natural polyphenols including formulation standardization and batch-to-batch variability. To address these translational bottlenecks, future research should focus on developing sustained-release

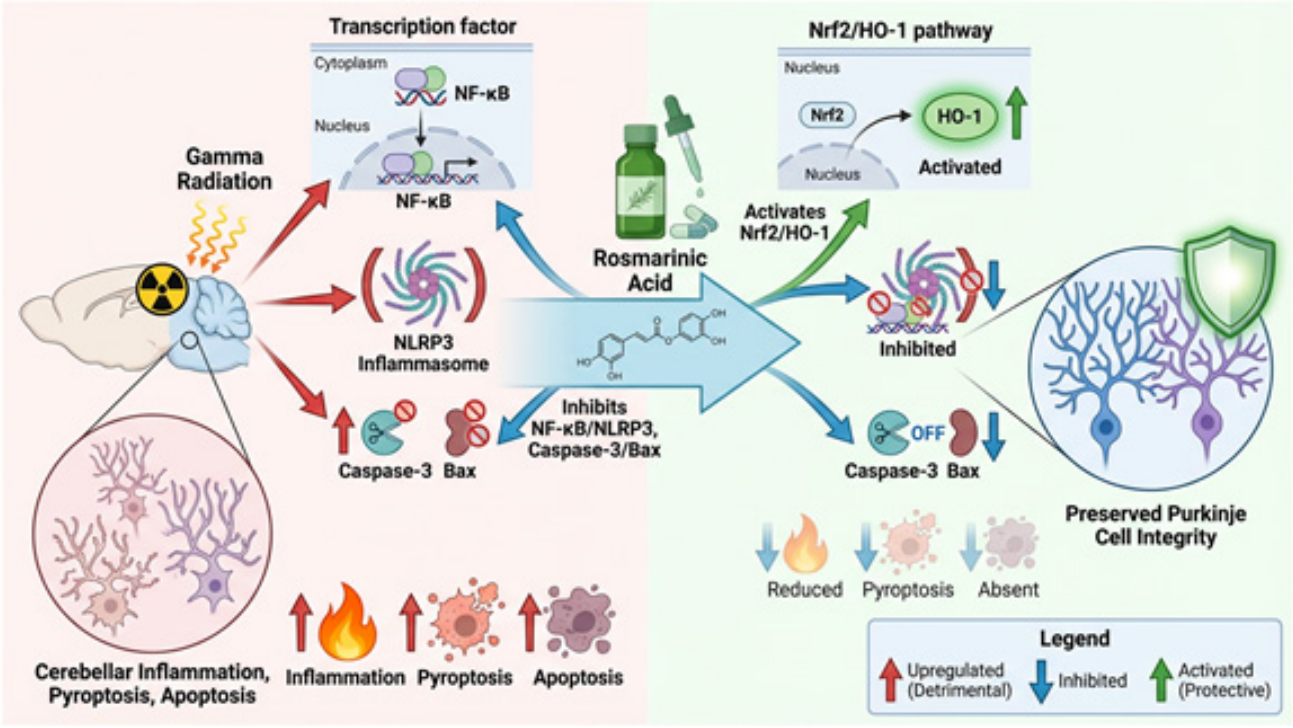


Fig. 9. Graphical abstract overviewing the hierarchical protective mechanism of RA. RA-driven Nrf2 activation acts as an upstream bottleneck, sequentially suppressing NF-κB priming, blocking NLRP3 inflammasome assembly, and downregulating Caspase-3/Bax. This regulatory cascade mitigates inflammation, pyroptosis, and apoptosis, leading to cerebellar Purkinje cell preservation (Red arrows: detrimental activation; Blue arrows: inhibition; Green arrows: protective activation). Created by FigDraw.

formulations, validating RA neuroprotection in fractionated RT models, and conducting pharmacokinetic, pharmacodynamic, and toxicity studies. Future studies employing Nrf2 knockout animals, siRNA-mediated knockdown, CRISPR/Cas9 gene editing in cerebellar cell lines, or specific pathway inhibitors would provide definitive confirmation of the causal role of these signaling cascades in RA-mediated neuroprotection. Future research incorporating fractionated irradiation protocols and sex-balanced designs will be essential to advance these findings toward clinical translation.

5. Conclusions

This study concluded that RA provides neuroprotection against GR-induced cerebellar toxicity. The protective effect is partially due to RA's potent antioxidant properties, demonstrated by reduced lipid peroxidation (MDA) and activation of the *Nrf2*/*HO-1* pathway, which led to increased levels of endogenous antioxidant enzymes. Moreover, RA exhibited strong anti-inflammatory activity by inhibiting the *NF-κB*/*NLRP3* signaling pathway, resulting in a marked reduction in inflammatory cytokines, including IL-18 and IL-1β, as well as the pyroptosis-associated protease caspase-1. Furthermore, RA showed anti-apoptotic effects in Purkinje cells, improving cerebellar histological architecture by downregulating *caspase-3* and *Bax* while upregulating *Bcl-2* expression. Collectively, these multi-index data outline a clear causal chain, as summarized in the Graphical Abstract, wherein RA-mediated Nrf2 activation acts as the upstream trigger to suppress NF-κB/NLRP3 priming, ultimately attenuating the downstream pyroptotic and apoptotic cascades to preserve Purkinje cell integrity (Fig. 9). These combined actions suggest that RA holds significant therapeutic potential for reducing the neuronal side effects of GR in cancer patients undergoing RT.

Abbreviations

ANOVA, Analysis of variance; ARE, Antioxidant response element; Bax, Bcl-2-associated X protein; Bcl-2, B-cell lymphoma 2; CAT, Catalase; cDNA, Complementary deoxyribonucleic acid; ELISA, Enzyme-linked immunosorbent assay; FR, Free radical; GAPDH, Glyceraldehyde-3-phosphate dehydrogenase; GFAP, Glial fibrillary acidic protein; GR, Gamma radiation; GSH, Glutathione; H&E, Hematoxylin and eosin; HO-1, Heme oxygenase-1; HRP, Horseradish peroxidase; IHC, Immunohistochemistry; IKKβ, Inhibitor of nuclear factor kappa-B kinase subunit beta; IL-1β, Interleukin-1 beta; IL-6, Interleukin-6; IL-18, Interleukin-18; IR, Ionizing radiation; Keap1, Kelch-like ECH-associated protein 1; MDA, Malondialdehyde; mRNA, Messenger ribonucleic acid; NF-κB, Nuclear factor kappa-B; NLRP3, NLR family pyrin domain-containing 3; NOD, Nucleotide-binding oligomerization domain; Nrf2, Nuclear factor erythroid 2-related

factor 2; PBS, Phosphate-buffered saline; PDB, Protein Data Bank; PUFA, Polyunsaturated fatty acid; qRT-PCR, Quantitative reverse transcription polymerase chain reaction; RA, Rosmarinic acid; ROS, Reactive oxygen species; rpm, Revolutions per minute; RT, Radiotherapy; SOD, Superoxide dismutase; TNF-α, Tumor necrosis factor-alpha.

Availability of Data and Materials

The data that support this research will be shared upon reasonable request to the corresponding author.

Author Contributions

AA: contributed to the interpretation of the data; MT: conceptualization; NFQ: data curation; BTB: investigation; TASB: methodology; OB: investigation; AJAA: data curation; TMA: contributed to the conception and design of the study. All authors contributed to critical revision of the manuscript for important intellectual content. All authors have read and agreed to the published version of the manuscript. All authors have participated sufficiently in the work and agreed to be accountable for all aspects of the work.

Ethics Approval and Consent to Participate

All animal protocols were approved by the Scientific Research Ethics Committee of Umm Al-Qura University, Makka, Saudi Arabia with approval number (HAPO-02-K-012-2025-06-2850). All animal experiments were conducted in accordance with the National Institutes of Health Guide for the Care and Use of Laboratory Animals and reported in accordance with the ARRIVE guidelines.

Acknowledgment

Not applicable.

Funding

This research received no external funding.

Conflicts of Interest

The authors declare no conflicts of interest.

Supplementary Material

Supplementary material associated with this article can be found, in the online version, at https://doi.org/10.31083/JIN55213.

References

[1] Sung H, Ferlay J, Siegel RL, Laversanne M, Soerjomataram I, Jemal A, et al. Global Cancer Statistics 2020: GLOBOCAN Estimates of Incidence and Mortality Worldwide for 36 Cancers in 185 Countries. CA: a Cancer Journal for Clinicians. 2021; 71: 209–249. https://doi.org/10.3322/caac.21660

[2] Bray F, Laversanne M, Sung H, Ferlay J, Siegel RL, Soerjomataram I, et al. Global cancer statistics 2022: GLOBOCAN estimates of incidence and mortality worldwide for 36 cancers in 185 countries. CA: a Cancer Journal for Clinicians. 2024; 74: 229–263. https://doi.org/10.3322/caac.21834

[3] Glynne-Jones R, Wyrwicz L, Tiret E, Brown G, Rödel C, Cervantes A, et al. Rectal cancer: ESMO Clinical Practice Guidelines for diagnosis, treatment and follow-up. Annals of Oncology. 2017; 28: iv22–iv40. https://doi.org/10.1093/annonc/mdx224

[4] Postmus PE, Kerr KM, Oudkerk M, Senan S, Waller DA, Vansteenkiste J, et al. Early and locally advanced non-small-cell lung cancer (NSCLC): ESMO Clinical Practice Guidelines for diagnosis, treatment and follow-up. Annals of Oncology. 2017; 28: iv1–iv21. https://doi.org/10.1093/annonc/mdx222

[5] Parker C, Gillessen S, Heidenreich A, Horwich A, ESMO Guidelines Committee. Cancer of the prostate: ESMO Clinical Practice Guidelines for diagnosis, treatment and follow-up. Annals of Oncology. 2015; 26: v69–v77. https://doi.org/10.1093/annonc/mdv222

[6] Delaney G, Jacob S, Featherstone C, Barton M. The role of radiotherapy in cancer treatment: estimating optimal utilization from a review of evidence-based clinical guidelines. Cancer. 2005; 104: 1129–1137. https://doi.org/10.1002/cncr.21324

[7] Bristow RG, Alexander B, Baumann M, Bratman SV, Brown JM, Camphausen K, et al. Combining precision radiotherapy with molecular targeting and immunomodulatory agents: a guideline by the American Society for Radiation Oncology. The Lancet. Oncology. 2018; 19: e240–e251. https://doi.org/10.1016/S1470-2045(18)30096-2

[8] Wei W, Ren Y, Lan J, Yi J, Wang M, Zhang Y, et al. Ionizing radiation: molecular mechanisms, biological effects, and therapeutic targets. Molecular Biomedicine. 2026; 7: 3. https://doi.org/10.1186/s43556-025-00358-4

[9] Piraux E, Caty G, Aboubakar Nana F, Reychler G. Effects of exercise therapy in cancer patients undergoing radiotherapy treatment: a narrative review. SAGE Open Medicine. 2020; 8: 2050312120922657. https://doi.org/10.1177/2050312120922657

[10] Klaus R, Niyazi M, Lange-Sperandio B. Radiation-induced kidney toxicity: molecular and cellular pathogenesis. Radiation Oncology (London, England). 2021; 16: 43. https://doi.org/10.1186/s13014-021-01764-y

[11] Schaue D, McBride WH. Opportunities and challenges of radiotherapy for treating cancer. Nature Reviews. Clinical Oncology. 2015; 12: 527–540. https://doi.org/10.1038/nrclinonc.2015.120

[12] Bowen J, Gregory R, Squier M, Donaghy M. The post-irradiation lower motor neuron syndrome neuronopathy or radiculopathy? Brain: a Journal of Neurology. 1996; 119: 1429–1439. https://doi.org/10.1093/brain/119.5.1429

[13] Greene-Schloesser D, Robbins ME, Peiffer AM, Shaw EG, Wheeler KT, Chan MD. Radiation-induced brain injury: A review. Frontiers in Oncology. 2012; 2: 73. https://doi.org/10.3389/fonc.2012.00073

[14] Schmitz C, Born M, Dolezel P, Rutten BPF, de Saint-Georges L, Hof PR, et al. Prenatal protracted irradiation at very low dose rate induces severe neuronal loss in rat hippocampus and cerebellum. Neuroscience. 2005; 130: 935–948. https://doi.org/10.1016/j.neuroscience.2004.08.034

[15] Lee HJ, Kim SR, Kim JC, Kang CM, Lee YS, Jo SK, et al. In Vivo radioprotective effect of Panax ginseng C.A. Meyer and identification of active ginsenosides. Phytotherapy Research: PTR. 2006; 20: 392–395. https://doi.org/10.1002/ptr.1867

[16] Aruoma OI. Free radicals, oxidative stress, and antioxidants in human health and disease. Journal of the American Oil Chemists' Society. 1998; 75: 199–212. https://doi.org/10.1007/s11746-998-0032-9

[17] O'Connor MM, Mayberg MR. Effects of radiation on cerebral

vasculature: a review. Neurosurgery. 2000; 46: 138–151. https://doi.org/10.1093/neurosurgery/46.1.138
[18] Belka C, Budach W, Kortmann RD, Bamberg M. Radiation induced CNS toxicity–molecular and cellular mechanisms. British Journal of Cancer. 2001; 85: 1233–1239. https://doi.org/10.1054/bjoc.2001.2100
[19] Wang H, Sim MK, Loke WK, Chinnathambi A, Alharbi SA, Tang FR, et al. Potential Protective Effects of Ursolic Acid against Gamma Irradiation-Induced Damage Are Mediated through the Modulation of Diverse Inflammatory Mediators. Frontiers in Pharmacology. 2017; 8: 352. https://doi.org/10.3389/fphar.2017.00352
[20] Yu H, Aravindan N, Xu J, Natarajan M. Inter- and intra-cellular mechanism of NF-kB-dependent survival advantage and clonal expansion of radio-resistant cancer cells. Cellular Signalling. 2017; 31: 105–111. https://doi.org/10.1016/j.cellsig.2017.01.011
[21] Li F, Sethi G. Targeting transcription factor NF-kappaB to overcome chemoresistance and radioresistance in cancer therapy. Biochimica et Biophysica Acta. 2010; 1805: 167–180. https://doi.org/10.1016/j.bbcan.2010.01.002
[22] Sethi G, Tergaonkar V. Potential pharmacological control of the NF-κB pathway. Trends in Pharmacological Sciences. 2009; 30: 313–321. https://doi.org/10.1016/j.tips.2009.03.004
[23] Stoecklein VM, Osuka A, Ishikawa S, Lederer MR, Wanke-Jellinek L, Lederer JA. Radiation exposure induces inflammasome pathway activation in immune cells. Journal of Immunology (Baltimore, Md.: 1950). 2015; 194: 1178–1189. https://doi.org/10.4049/jimmunol.1303051
[24] Cheng YC, Chu LW, Chen JY, Hsieh SL, Chang YC, Dai ZK, et al. Loganin Attenuates High Glucose-Induced Schwann Cells Pyroptosis by Inhibiting ROS Generation and NLRP3 Inflammasome Activation. Cells. 2020; 9: 1948. https://doi.org/10.3390/cells9091948
[25] He F, Antonucci L, Karin M. NRF2 as a regulator of cell metabolism and inflammation in cancer. Carcinogenesis. 2020; 41: 405–416. https://doi.org/10.1093/carcin/bgaa039
[26] Li H, Zhang J, Yu B, Yang T, Liu B, Li F, et al. RSPO3 regulates the radioresistance of Non-Small cell lung cancer cells via NLRP3 Inflammasome-Mediated pyroptosis. Radiotherapy and Oncology: Journal of the European Society for Therapeutic Radiology and Oncology. 2024; 200: 110528. https://doi.org/10.1016/j.radonc.2024.110528
[27] Zhang M, Lan H, Jiang M, Yang M, Chen H, Peng S, et al. NLRP3 inflammasome mediates pyroptosis of alveolar macrophages to induce radiation lung injury. Journal of Hazardous Materials. 2025; 484: 136740. https://doi.org/10.1016/j.jhazmat.2024.136740
[28] Makino T, Ono T, Muso E, Honda G. Inhibitory effect of Perilla frutescens and its phenolic constituents on cultured murine mesangial cell proliferation. Planta Medica. 1998; 64: 541–545. https://doi.org/10.1055/s-2006-957510
[29] Jiang K, Ma X, Guo S, Zhang T, Zhao G, Wu H, et al. Anti-inflammatory Effects of Rosmarinic Acid in Lipopolysaccharide-Induced Mastitis in Mice. Inflammation. 2018; 41: 437–448. https://doi.org/10.1007/s10753-017-0700-8
[30] Sotnikova R, Okruhlicova L, Vlkovicova J, Navarova J, Gajdacova B, Pivackova L, et al. Rosmarinic acid administration attenuates diabetes-induced vascular dysfunction of the rat aorta. The Journal of Pharmacy and Pharmacology. 2013; 65: 713–723. https://doi.org/10.1111/jphp.12037
[31] González-Vallinas M, Reglero G, Ramírez de Molina A. Rosemary (Rosmarinus officinalis L.) Extract as a Potential Complementary Agent in Anticancer Therapy. Nutrition and Cancer. 2015; 67: 1221–1229. https://doi.org/10.1080/01635581.2015.1082110
[32] Lee HJ, Cho HS, Park E, Kim S, Lee SY, Kim CS, et al. Rosmarinic acid protects human dopaminergic neuronal cells against hydrogen peroxide-induced apoptosis. Toxicology. 2008; 250: 109–115. https://doi.org/10.1016/j.tox.2008.06.010
[33] Wang H, Provan GJ, Helliwell K. Determination of rosmarinic and caffeic acids in herbs by HPLC. Food Chemistry. 2004; 87: 307–311. https://doi.org/10.1016/j.foodchem.2003.12.029
[34] Tavafi M. Diabetic nephropathy and antioxidants. Journal of Nephropathology. 2013; 2: 20–27. https://doi.org/10.5812/nephropathol.9093
[35] Xu W, Yang F, Zhang Y, Shen X. Protective effects of rosmarinic acid against radiation-induced damage to the hematopoietic system in mice. Journal of Radiation Research. 2016; 57: 356–362. https://doi.org/10.1093/jrr/rrw021
[36] Khateeb S. Etoricoxib-NLC Mitigates Radiation-Induced Ovarian Damage in Rats: Insights into Pro-Inflammatory Cytokines, Antioxidant Activity, and Hormonal Responses. Biomolecules. 2024; 15: 12. https://doi.org/10.3390/biom15010012
[37] Zhang T, Liu C, Ma S, Gao Y, Wang R. Protective Effect and Mechanism of Action of Rosmarinic Acid on Radiation-Induced Parotid Gland Injury in Rats. Dose-response: a Publication of International Hormesis Society. 2020; 18: 1559325820907782. https://doi.org/10.1177/1559325820907782
[38] Deacon RMJ. Measuring motor coordination in mice. Journal of Visualized Experiments: JoVE. 2013; e2609. https://doi.org/10.3791/2609
[39] Oh SS, Narver HL. Mouse and Rat Anesthesia and Analgesia. Current Protocols. 2024; 4: e99. https://doi.org/10.1002/cpz1.995
[40] Mihara M, Uchiyama M. Determination of malonaldehyde precursor in tissues by thiobarbituric acid test. Analytical Biochemistry. 1978; 86: 271–278. https://doi.org/10.1016/0003-2697(78)90342-1
[41] Marklund S, Marklund G. Involvement of the superoxide anion radical in the autoxidation of pyrogallol and a convenient assay for superoxide dismutase. European Journal of Biochemistry. 1974; 47: 469–474. https://doi.org/10.1111/j.1432-1033.1974.tb03714.x
[42] Oberley L, Spitz D. CRC handbook of methods for oxygen radical research. CRC Press: Boca Raton, FL. 1985.
[43] ELLMAN GL. Tissue sulfhydryl groups. Archives of Biochemistry and Biophysics. 1959; 82: 70–77. https://doi.org/10.1016/0003-9861(59)90090-6
[44] Zhang Z, Miah M, Culbreth M, Aschner M. Autophagy in Neurodegenerative Diseases and Metal Neurotoxicity. Neurochemical Research. 2016; 41: 409–422. https://doi.org/10.1007/s11064-016-1844-x
[45] Livak KJ, Schmittgen TD. Analysis of gene expression using qPCR and 2(-ΔΔCT) method. Methods. 2001; 25: 402–408. https://doi.org/10.1006/meth.2001.1262
[46] Wei J, Wang B, Wang H, Meng L, Zhao Q, Li X, et al. Radiation-Induced Normal Tissue Damage: Oxidative Stress and Epigenetic Mechanisms. Oxidative Medicine and Cellular Longevity. 2019; 2019: 3010342. https://doi.org/10.1155/2019/3010342
[47] Lord CJ, Ashworth A. The DNA damage response and cancer therapy. Nature. 2012; 481: 287–294. https://doi.org/10.1038/nature10760
[48] Kale A, Pişkin O, Baş Y, Aydın BG, Can B, Buyukuysa C. Ameliorative effects of hesperidin on radiation-induced brain injury in rats. International Journal of Radiation Research. 2019; 17: 229–236. https://doi.org/10.18869/acadpub.ijrr.17.2.229
[49] Abd-Al-Haleem EN, Eldeen-Hussein SS, Fahmy HAH, Mahmoud-Taha RA. Effect of gamma radiation on combination therapy of certain antiepileptic drugs in rats. Pakistan Journal of Pharmaceutical Sciences. 2019; 32: 1589–1597.

[50] Soliman AM, Karam HM, Mekkawy MH, Higgins M, Dinkova-Kostova AT, Ghorab MM. Radiomodulatory effect of a non-electrophilic NQO1 inducer identified in a screen of new 6, 8-diiodoquinazolin-4(3H)-ones carrying a sulfonamide moiety. European Journal of Medicinal Chemistry. 2020; 200: 112467. https://doi.org/10.1016/j.ejmech.2020.112467

[51] Karaca O, Şimşek H, Akaras N, Gür C, İleritürk M, Kandemir Ö, et al. Potent Ameliorative Effects of Rosmarinic Acid on Tramadol-Induced Neurotoxicity in the Brain and Hippocampus; by Suppressing Oxidative stress, Apoptosis, ER stress, and Regulating Cognitive Functions. Molecular Neurobiology. 2025; 62: 10245–10263. https://doi.org/10.1007/s12035-025-04892-8

[52] Fadel O, El Kirat K, Morandat S. The natural antioxidant rosmarinic acid spontaneously penetrates membranes to inhibit lipid peroxidation in situ. Biochimica et Biophysica Acta. 2011; 1808: 2973–2980. https://doi.org/10.1016/j.bbamem.2011.08.011

[53] Truong DH, Ngo TC, Nhung NTA, Quang DT, Nguyen TLA, Khiri D, et al. New insights into the competition between antioxidant activities and pro-oxidant risks of rosmarinic acid. RSC Advances. 2022; 12: 1499–1514. https://doi.org/10.1039/d1ra07599c

[54] Li B, Nasser MI, Masood M, Adlat S, Huang Y, Yang B, et al. Efficiency of Traditional Chinese medicine targeting the Nrf2/HO-1 signaling pathway. Biomedicine & Pharmacotherapy = Biomedecine & Pharmacotherapie. 2020; 126: 110074. https://doi.org/10.1016/j.biopha.2020.110074

[55] Zhang T, Shi L, Li Y, Mu W, Zhang H, Li Y, et al. Polysaccharides extracted from Rheum tanguticum ameliorate radiation-induced enteritis via activation of Nrf2/HO-1. Journal of Radiation Research. 2021; 62: 46–57. https://doi.org/10.1093/jrr/rraa093

[56] Cui HY, Zhang XJ, Yang Y, Zhang C, Zhu CH, Miao JY, et al. Rosmarinic acid elicits neuroprotection in ischemic stroke via Nrf2 and heme oxygenase 1 signaling. Neural Regeneration Research. 2018; 13: 2119–2128. https://doi.org/10.4103/1673-5374.241463

[57] Shim KS, Kim HJ, Ji KY, Jung DH, Park SH, Song HK, et al. Rosmarinic Acid Ameliorates Dermatophagoides farinae Extract-Induced Atopic Dermatitis-like Skin Inflammation by Activating the Nrf2/HO-1 Signaling Pathway. International Journal of Molecular Sciences. 2024; 25: 12737. https://doi.org/10.3390/ijms252312737

[58] Mariotti LG, Bertolotti A, Ranza E, Babini G, Ottolenghi A. Investigation of the mechanisms underpinning IL-6 cytokine release in bystander responses: the roles of radiation dose, radiation quality and specific ROS/RNS scavengers. International Journal of Radiation Biology. 2012; 88: 751–762. https://doi.org/10.3109/09553002.2012.703365

[59] Hellweg CE, Baumstark-Khan C, Schmitz C, Lau P, Meier MM, Testard I, et al. Carbon-ion-induced activation of the NF-κB pathway. Radiation Research. 2011; 175: 424–431. https://doi.org/10.1667/RR2423.1

[60] Chishti AA, Baumstark-Khan C, Hellweg CE, Reitz G. Imaging of nuclear factor κB activation induced by ionizing radiation in human embryonic kidney (HEK) cells. Radiation and Environmental Biophysics. 2014; 53: 599–610. https://doi.org/10.1007/s00411-014-0541-x

[61] Sivandzade F, Prasad S, Bhalerao A, Cucullo L. NRF2 and NF-κB interplay in cerebrovascular and neurodegenerative disorders: Molecular mechanisms and possible therapeutic approaches. Redox Biology. 2019; 21: 101059. https://doi.org/10.1016/j.redox.2018.11.017

[62] Lee WH, Sonntag WE, Mitschelen M, Yan H, Lee YW. Irradiation induces regionally specific alterations in pro-inflammatory environments in rat brain. International Journal of Radiation Biology. 2010; 86: 132–144. https://doi.org/10.3109/09553000903419346

[63] Wilke C, Grosshans D, Duman J, Brown P, Li J. Radiation-induced cognitive toxicity: pathophysiology and interventions to reduce toxicity in adults. Neuro-oncology. 2018; 20: 597–607. https://doi.org/10.1093/neuonc/nox195

[64] Jha MK, Jo M, Kim JH, Suk K. Microglia-Astrocyte Crosstalk: An Intimate Molecular Conversation. The Neuroscientist: a Review Journal Bringing Neurobiology, Neurology and Psychiatry. 2019; 25: 227–240. https://doi.org/10.1177/1073858418783959

[65] Chen SH, Oyarzabal EA, Sung YF, Chu CH, Wang Q, Chen SL, et al. Microglial regulation of immunological and neuroprotective functions of astroglia. Glia. 2015; 63: 118–131. https://doi.org/10.1002/glia.22738

[66] Wang L, Li C, Sreeharsha N, Mishra A, Shrotriya V, Sharma A. Neuroprotective effect of Wogonin on Rat's brain exposed to gamma irradiation. Journal of Photochemistry and Photobiology. B, Biology. 2020; 204: 111775. https://doi.org/10.1016/j.jphotobiol.2020.111775

[67] He B, Wang X, He Y, Li H, Yang Y, Shi Z, et al. Gamma ray-induced glial activation and neuronal loss occur before the delayed onset of brain necrosis. FASEB Journal. 2020; 34: 13361–13375. https://doi.org/10.1096/fj.202000365RR

[68] Lee J, Jung E, Kim Y, Lee J, Park J, Hong S, et al. Rosmarinic acid as a downstream inhibitor of IKK-beta in TNF-alpha-induced upregulation of CCL11 and CCR3. British Journal of Pharmacology. 2006; 148: 366–375. https://doi.org/10.1038/sj.bjp.0706728

[69] Ahmed SMU, Luo L, Namani A, Wang XJ, Tang X. Nrf2 signaling pathway: Pivotal roles in inflammation. Biochimica et Biophysica Acta. Molecular Basis of Disease. 2017; 1863: 585–597. https://doi.org/10.1016/j.bbadis.2016.11.005

[70] Smith AO, Ju W, Adzraku SY, Wenyi L, Yuting C, Qiao J, et al. Gamma Radiation Induce Inflammasome Signaling and Pyroptosis in Microvascular Endothelial Cells. Journal of Inflammation Research. 2021; 14: 3277–3288. https://doi.org/10.2147/JIR.S318812

[71] Mohamed M, Ahmed M. Apoptotic genes expression in γ-irradiated rats treated with wheat germ oil, zinc and /or bone marrow. International Journal of Basic and Applied Sciences. 2014; 3: 451. https://doi.org/10.14419/ijbas.v3i4.3657

[72] Kouvaris JR, Kouloulias VE, Vlahos LJ. Amifostine: the first selective-target and broad-spectrum radioprotector. The Oncologist. 2007; 12: 738–747. https://doi.org/10.1634/theoncologist.12-6-738

[73] Hensley ML, Hagerty KL, Kewalramani T, Green DM, Meropol NJ, Wasserman TH, et al. American Society of Clinical Oncology 2008 clinical practice guideline update: use of chemotherapy and radiation therapy protectants. Journal of Clinical Oncology. 2009; 27: 127–145. https://doi.org/10.1200/JCO.2008.17.2627

[74] Petersen M, Simmonds MSJ. Rosmarinic acid. Phytochemistry. 2003; 62: 121–125. https://doi.org/10.1016/s0031-9422(02)00513-7